CAPTURE COEFFICIENTS OF NITROGEN ON A CRYOGENICALLY COOLED PANEL

JOHN ALBERT BEVAN

CAPTURE COEFFICIENTS OF NITROGEN ON A CRYOGENICALLY COOLED PANEL

by

John Albert Bevan
Lieutenant Commander, United States Navy
B. S., Pennsylvania State University, 1957

Submitted in partial fulfillment of the
requirements for the degree of

MASTER OF SCIENCE IN MECHANICAL ENGINEERING

from the

NAVAL POSTGRADUATE SCHOOL
June 1967

ABSTRACT

The pressure drop method was used to experimentally determine the capture coefficients of nitrogen gas on a flat cryopanel maintained at a temperature of 25°K. The capture coefficients for 300°K nitrogen varied from a maximum of 0.70 for low system gas loads to a minimum of 0.10 for high system gas loads.

TABLE OF CONTENTS

TABLES

LIST OF ILLUSTRATIONS

LIST OF SYMBOLS

A	surface area	cm^2
A_s	cryosurface area	cm^2
C	conductance constant	
f	capture coefficient	
f_g	condensation coefficient	
f_s	evaporation coefficient	
k	Boltzmann constant	erg $°K^{-1}$
K_n	Knudson number	
M	molecular weight	gm $(gm.mole)^{-1}$
m	mass of a molecule	gm
n	number of molecules per unit volume	cm^{-3}
N	total number of molecules	
N_A	Avagadro's number	
$\dot{N}$	number of molecules per unit time	sec^{-1}
$\dot{N}_a$	summation of molecular flow into V_a	sec^{-1}
$\dot{N}_{ai}$	flow of molecules from V_a to V_i	sec^{-1}
$\dot{N}_D$	flow of molecules to diffusion pump	sec^{-1}
$\dot{N}_i$	summation of molecular flow into V_i	sec^{-1}
$\dot{N}_{io}$	flow of molecules from V_i to V_o	sec^{-1}
$\dot{N}_L$	flow of molecules into V_a from gas addition system	sec^{-1}
$\dot{N}_o$	summation of molecular flow into V_o	sec^{-1}
$\dot{N}_r$	flow of residual gas molecules	sec^{-1}
P	total pressure	torr
$\dot{P}$	pressure per unit time	torr sec^{-1}
P_e	chamber equilibrium pressure with gas flow on	torr
P_g	chamber equilibrium pressure with no gas flow	torr
P_i	pressure in V_i	torr

P_L	pressure at entrance to V_a	torr
P_o	pressure in V_o	torr
P_t	transition pressure	torr
Q_L	throughput rate	torr liter sec^{-1}
R	universal gas constant	erg $°K^{-1}$ $gm\text{-}mole^{-1}$
S_{th}	theoretical pumping speed	liter sec^{-1} cm^{-2}
T	absolute temperature	°K
T_a	temperature in V_a	°K
T_g	gas temperature	°K
T_i	temperature in V_i	°K
T_L	temperature in V_L	°K
T_o	temperature in V_o	°K
T_s	temperature of the cryosurface	°K
$\bar{v}$	average molecular velocity	cm sec^{-1}
V	volume	cm^3
$\dot{V}$	volume per unit time	cm^3 sec^{-1}
V_a	volume of gas addition piping	cm^3
$\dot{V}_D$	diffusion pump volumetric flow rate	cm^3 sec^{-1}
V_i	volume within the radiation shielding	cm^3
V_L	volume of auxiliary vacuum system	cm^3
V_o	volume between shielding and chamber walls	cm^3
α	diffusion pump efficiency factor	
β	conductance area between V_o and V_i	cm^2
Φ	Maxwell-Boltzmann velocity distribution function	
μ	micron	
γ	correction factor	

ACKNOWLEDGEMENTS

The work described herein was made possible by the continued support of the Office of Naval Research through the Foundation Research Program.

The author wishes to express his gratitude to Professor Paul F. Pucci for his continued support and encouragement. He also wishes to thank Mr. K. Mothersell for his helpful assistance and especially Messrs. J. Beck and K. Smith for their generous and enthusiastic assistance.

1. Introduction.

Simulation of the environment of outer space and experiments in high energy nuclear physics and on controlled thermonuclear fusion require the production and maintenance of an ultrahigh vacuum. Ultrahigh vacuum may be classified as the range of pressures from about 10^{-8} torr to 10^{-13} torr (1) where one torr is equivalent to the pressure exerted by a column of mercury one millimeter high. The most important parameters to be considered in the design of an ultrahigh vacuum system are the expected gas load in terms of quantities of various component gases and the operating pressure at which a particular process is to be carried out. Ultrahigh vacuum systems generally use some combination of mechanical and vapor-jet vacuum pumps along with ion pumps, cryopumps or cryosorption pumps. For systems with very little gas load, low pressure can be obtained by suitable bakeout to reduce outgassing and the subsequent utilization of low pump speeds. Generally oil diffusion pumps, suitably trapped, will suffice. In fact it was shown that a thoroughly outgassed system can be maintained in the ultrahigh vacuum range by the pumping action of an ionization gage alone when closed off from the vacuum pump by a sufficiently tight bakable valve (2). This type of system is essentially static in that ultrahigh vacuum is maintained on a small scale with almost zero gas load.

Controlled fusion research and space simulation require large volumes and generate appreciable gas loads thus requiring vacuum systems that have high pumping speeds at low pressures. For example, in a space simulation chamber, the system must be capable of handling the high gas loads generated by the test firing of vehicle control rockets and must still maintain base pressures of about 10^{-8} torr. The use of mechanical and diffusion pumps alone becomes prohibitively expensive because of the large sizes required in order to achieve the high pumping speeds. A diffusion

pump capable of pumping 95,000 liters per second at 10^{-8} torr is 48 inches in diameter and weights 3320 pounds. A cryopump with a surface area of only 14.3 square feet can pump 95,000 liters per second of nitrogen gas at 300°K with 60% efficiency at a pump temperature of 20°K. The walls of the vacuum chamber itself can be used as the cryopump thereby eliminating large pump suction ports in the system with the attendant problems of adequately sealing these openings against leakage.

Cryopumping consists of exposing surfaces maintained at low temperatures to the gases in a vacuum chamber so that the gases condense as long as their partial pressures are above the equilibrium vapor pressure at the temperature of the condensing surface. Liquefied gases such as helium and nitrogen provide a convenient means of obtaining these cold surfaces. Although the concept of cryopumping is not new, the need for high pumping speeds at low pressures has greatly increased the development of cryopumping systems. This development has been greatly aided by the rapid growth of the cryogenics industry to meet the need for large quantities of liquid oxygen, nitrogen, hydrogen and helium required by the various space systems.

In order to make quantitative judgements concerning the performance of a cryopump, it is necessary to predict the ability of a cold surface to freeze condensable gases. The measure of cryopump performance is the capture or sticking coefficient which is generally defined as the probability that a gas molecule will condense on a cold surface in its first collision with that surface. A theoretical understanding of the interaction of the gas and condensate molecules at the solid-gas interface is still to be achieved. Consequently, a prediction of the area of pumping surface required to remove a gas cannot be made unless the capture coefficient of that gas has already been experimentally determined.

Although data concerning capture coefficients are not abundant, efforts have been and are being made to obtain such data. Experiments have been conducted to ascertain the effect of such parameters as gas temperature, cryosurface temperature, pressure, molecular weight, thickness, density and thermal conductivity of the condensate layer, Debye characteristic temperature, dipole moment and heat of condensation (3,4,5,6,7,8).

Hopefully, a continuing study at the Naval Postgraduate School will add to the understanding and measurement of the cryopumping phenomenon.

2. Cryopumping.

The vapor pressure of a solidified gas can be represented by an equation of the form

$$\text{Log}_{10}P = A - B/T \qquad (2.1)$$

where T is the absolute temperature and A and B are constants. Thus a plot of the logarithm of the vapor pressure versus the reciprocal of the absolute temperature is a straight line as shown in Figure 1. These curves reveal some of the advantages and limitations of cryopumping. For example, if a cryopump can be maintained at 20.4°K, then it can theoretically pump nitrogen to a pressure equal to the vapor pressure of about 5×10^{-10} torr. On the other hand, the cryopump must be maintained at a much lower temperature in order to pump neon into the ultrahigh vacuum range. The vapor pressure of hydrogen is even higher so that even at liquid helium temperatures (4.2°K), the vapor pressure is about 3×10^{-7} torr and rises rapidly with temperature. Helium is not even shown on the graph. Since the vapor pressure of helium is equal to atmospheric pressure at a temperature of only 4.2°K, cryopumping of helium is not feasible at temperatures which can practically be obtained today.

Temperatures which can be conveniently maintained and are frequently used for cryopumping are those corresponding to the boiling points of common gases at atmospheric pressure. These temperatures are for helium 4.2°K; for hydrogen 20.4°K; for neon 27.3°K; and for nitrogen 77.4°K. Usually liquid helium and liquid hydrogen are used to maintain the surfaces at the desired condensing temperature and liquid nitrogen is used to cool radiation shields placed between the cryopump and the room temperature wall of the vacuum chamber. This shielding helps to reduce the evaporation loss of the liquid helium or hydrogen by radiative heat

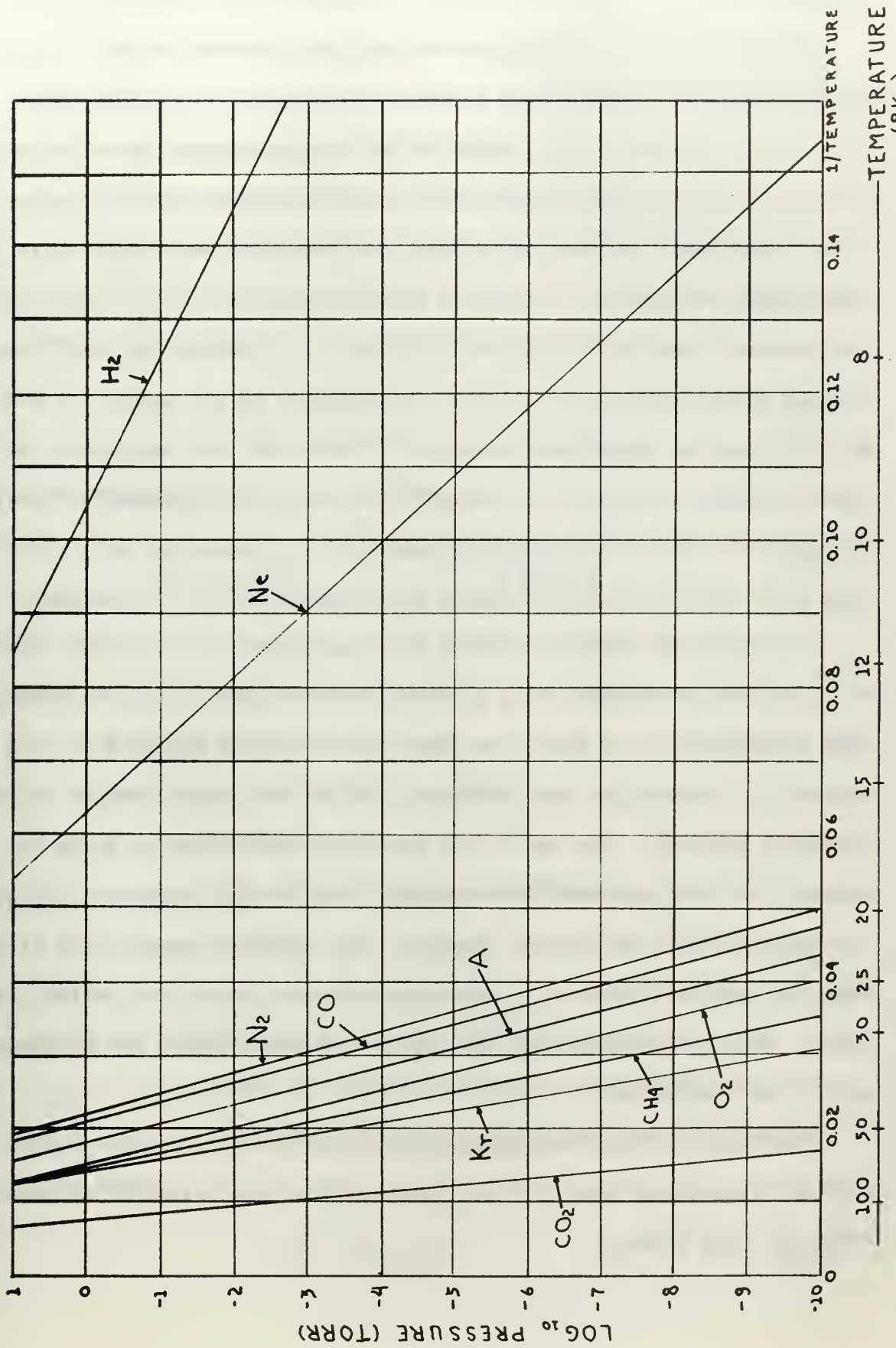

FIGURE 1. VAPOR PRESSURE OF VARIOUS GASES

transfer and thus reduces the amount of liquid helium or hydrogen required.

The use of only a cryopump to achieve low pressures is not feasible. If a cryopump at a temperature of 30°K were used to evacuate a chamber filled with atmospheric air, three of the component gases of air, namely helium, neon and hydrogen would not be condensed by the cooled surface. These gases would continue to collide with the room temperature walls of the chamber and maintain a pressure of approximately 2×10^{-2} torr within the chamber. Another limitation on the use of a cryopump by itself occurs because of the build up of a layer of condensate on the surface of the pump. As this layer of condensate increases in thickness, the temperature at the outer surface increases and eventually the pump must be warmed in order to melt the condensate. At high pressures, the condensate layer will grow more rapidly and more frequent warming periods will be required.

To reduce the effects of these two limitations, it is normal practice to first pump the chamber to a pressure as low as possible with a combination of mechanical and diffusion pumps. The ultimate pressure of such a system is a function of the diffusion pump and the vapor pressure of the diffusion pump oil. The use of the mechanical and diffusion pumps increases the time required for condensate build up and therefore decreases the number of warm up periods required. The diffusion pump should also keep the partial pressures of the non-condensable gases at a suitably low value. When the pressure has been reduced in this manner, the cryopump is put into operation.

The use of all of the pumping methods mentioned plus other methods such as cryosorption have led to pressures which are beginning to approach those of outer space.

3. Kinetic Theory of Gases.

The relationships of the kinetic theory of gases are used repeatedly in describing vacuum systems and the cryopumping phenomenom. They are presented here for reference.

a. Average molecular velocity.

The Maxwell-Boltzman velocity distribution function is defined as the fractional number of molecules in the velocity range from v to v + dv per unit of velocity range and is

$$\Phi = \frac{4}{\sqrt{\pi}}\left(\frac{m}{2kT}\right)v^2 \exp\left(-\frac{mv^2}{2kT}\right) \qquad (3.1)$$

The average velocity is therefore

$$\bar{V} = \frac{\int_0^\infty v\Phi\, dv}{\int_0^\infty \Phi\, dv} = \left(\frac{8kT}{\pi m}\right)^{1/2} \qquad (3.2)$$

where k = Boltzman constant, ergs/°K

T = absolute temperature, °K

m = mass of one molecule, grams.

b. Pressure.

The pressure within a chamber is

$$P = 1/3\, n m \bar{V}^2 \qquad (3.3)$$

where n = number of molecules per unit volume, cm^{-3}.

c. Number of molecules incident on a surface.

The number of molecules incident on a surface per unit time is

$$\dot{N} = 1/4\, A n \bar{V} \qquad (3.4)$$

where $\dot{N}$ = number of molecules per unit time, sec^{-1}

A = area of the surface, cm^2.

The ideal gas law may be expressed as

$$PV = NkT \tag{3.5}$$

where V = volume, cm^3

N = total number of molecules present.

Substitution of (3.2) and (3.5) into (3.4) yields

$$\dot{N} = \frac{PA}{(2\pi mkT)^{1/2}} \tag{3.6}$$

d. Thermal Transpiration.

If two volumes containing the same gas are connected by an aperture of area A and the temperatures of the two volumes are different, then the flow from volume 1 to volume 2 is

$$\dot{N}_{12} = \frac{P_1 A}{(2\pi mkT_1)^{1/2}} \tag{3.7}$$

and that from volume 2 to volume 1 is

$$\dot{N}_{21} = \frac{P_2 A}{(2\pi mkT_2)^{1/2}} \tag{3.8}$$

After a sufficient interval of time, equilibrium is established and these two flow rates become equal

$$\frac{P_1 A}{(2\pi mkT_1)^{1/2}} = \frac{P_2 A}{(2\pi mkT_2)^{1/2}} \tag{3.9}$$

or

$$\frac{P_1}{(T_1)^{1/2}} = \frac{P_2}{(T_2)^{1/2}} \tag{3.9}$$

This is the thermal transpiration effect. In the free molecular flow region, with no net flow, the ratio of the pressure to the square root of the temperature is a constant for different parts of a system.

e. Theoretical Pumping Speed

If every gas molecule that hits a surface remains there, the surface may be thought of as a pump and its theoretical specific pumping speed may be defined as

$$S_{th} = \frac{\dot{V}}{A} \tag{3.10}$$

where $\dot{V}$ = volume per unit time, $cm^3\ sec^{-1}$.

Substitution of the ideal gas law into (3.10) yields

$$S_{th} = \left(\frac{kT}{2\pi m}\right)^{1/2} \tag{3.11}$$

but

$$k = \frac{R}{N_A} \tag{3.12}$$

and

$$m = \frac{M}{N_A} \tag{3.13}$$

where R = universal gas constant, erg/gm-mole °K

N_A = Avagardro's number, $(\text{gm-mole})^{-1}$

M = molecular weight, gm/gm-mole.

Therefore (3.11) may be expressed as

$$S_{th} = \left(\frac{RT}{2\pi M}\right)^{1/2} \tag{3.14}$$

4. Definition of the Capture Coefficient.

The capture coefficient is defined as the ratio of the actual number of molecules captured by a cold surface to the theoretical maximum number which could be captured. It may also be thought of as the probability that a gas molecule will adhere to a surface on its first encounter with that surface. The following treatment is general and follows closely that of Haygood and Dawson (6).

In a vacuum chamber containing a cryosurface, the maximum possible volumetric pumping rate can be obtained from (3.14) as

$$\dot{V}_{th} = A_s S_{th} = A_s \left(\frac{RT_g}{2\pi M}\right)^{1/2} \tag{4.1}$$

where the subscript "g" refers to the gas and "s" to the cryosurface. If a gas load is imposed on the chamber through a controlled leak, then by continuity

$$\frac{R_L \dot{V}_L}{RT_L} = \frac{P\dot{V}}{RT_g} + \frac{V\dot{P}}{RT_g} \tag{4.2}$$

where the subscript "L" refers to conditions at the controlled leak. The left-hand side of the equation represents the amount of gas admitted through the leak and the right-hand side represents the amount of gas condensed per second. If the chamber reaches an equilibrium pressure P_e, then $\dot{P}$ is zero and

$$\frac{R_L \dot{V}_L}{RT_L} = \frac{P_e \dot{V}}{RT_g} \tag{4.3}$$

Defining the experimental pumping speed as $\dot{V}$ and the gas throughout Q_L as $P_L\dot{V}_L$, then

$$S_{exp} = \dot{V} = \frac{Q_L T_g}{P_e T_L} \qquad (4.4)$$

The capture coefficient, f, is then defined as

$$f = \frac{\dot{V}}{\dot{V}_{th}} = \frac{Q_L T_g}{P_e A_s T_L}\left(\frac{2\pi M}{R T_g}\right)^{1/2} \qquad (4.5)$$

The capture coefficient may be related to the condensation coefficient in the following manner.

a. `Isothermal enclosure.

If a pure condensed gas is placed in an isothermal enclosure, the vapor will be in equilibrium with the condensate and will have a pressure equal to the vapor pressure. If this pressure is low enough so that free molecular flow exists, then from kinetic theory, the number of molecules of vapor incident on the condensate is

$$\dot{N} = \frac{P_v A}{(2\pi m k T)^{1/2}} \qquad (4.6)$$

A certain fraction f of these molecules will condense and the rest will be reflected. Since the vapor is in equilibrium with the condensate, then the number of molecules condensed will be equal to the number which evaporate and there will be no net transfer of mass or energy.

$$\dot{N}_{cond} = \dot{N}_{evap}$$

or

$$\left(\frac{f P_v}{\sqrt{T}}\right)_{cond} = \left(\frac{f P_v}{\sqrt{T}}\right)_{evap} \tag{4.7}$$

b. Non-isothermal enclosure

If a temperature difference is maintained between the vapor and the condensate, then the rates of condensation and evaporation may be expressed as

$$\dot{N}_{cond} = \frac{f_g P_g A_s}{(2\pi m k T_g)^{1/2}} \tag{4.8}$$

$$\dot{N}_{evap} = \frac{f_s P_s A_s}{(2\pi m k T_s)^{1/2}} \tag{4.9}$$

where the subscript "g" refers to the gas and "s" refers to the condensate surface. f_g and f_s are the condensation and evaporation coefficients respectively, and represent the ratio of actual molecular flux to theoretical molecular flux.

In this case at equilibrium, the two rates will be equal and there will be an energy transfer due to the temperature difference. At equilibrium, the evaporation and condensation coefficients are related through the thermal transpiration effect and

$$\frac{f_g P_g}{\sqrt{T_g}} = \frac{f_s P_s}{\sqrt{T_s}} \tag{4.10}$$

c. Capture Coefficient with gas flow.

If a continuous stream of the gas is now injected into the enclosure, equilibrium will be achieved at a different pressure P_e,

when the rate at which molecules are captured by the cryosurface is equal to the rate at which they enter the enclosure. Therefore the difference between the actual condensation and evaporation rates is

$$\dot{N}_{act} = \frac{f_g P_e A_s}{(2\pi m k T_g)^{1/2}} - \frac{f_s P_s A_s}{(2\pi m k T_s)^{1/2}} \tag{4.11}$$

The theoretical rate of incidence of molecules on the surface is

$$\dot{N}_{th} = \frac{P_e A_s}{(2\pi m k T_g)^{1/2}} \tag{4.12}$$

The ratio of these two rates is the capture coefficient f and is

$$f = f_g \left(1 - \frac{f_s P_s \sqrt{T_g}}{f_g P_e \sqrt{T_s}} \right) \tag{4.13}$$

The evaporation coefficient is related to the condensation coefficient by (4.10) as

$$f_s = f_g \frac{P_g \sqrt{T_s}}{P_s \sqrt{T_g}} \tag{4.14}$$

and therefore

$$f = f_g \left(1 - \frac{P_g}{P_e} \right) \tag{4.15}$$

where P_g is the pressure of the gas with no flow into the enclosure and P_e is the equilibrium pressure established when a flow is admitted.

5. Experimental Determination of the Capture Coefficient.

5.1 Experimental Technique.

Figure 2 is a representation of the system used to determine the capture coefficient. A detailed description of the actual physical system is contained in Appendix A. The vacuum chamber is a stainless steel tank containing radiation shielding and the cryosurface. A combination of a forepump and a diffusion pump are used to accomplish the initial evacuation of the chamber. The cryosurface is cooled by cold helium

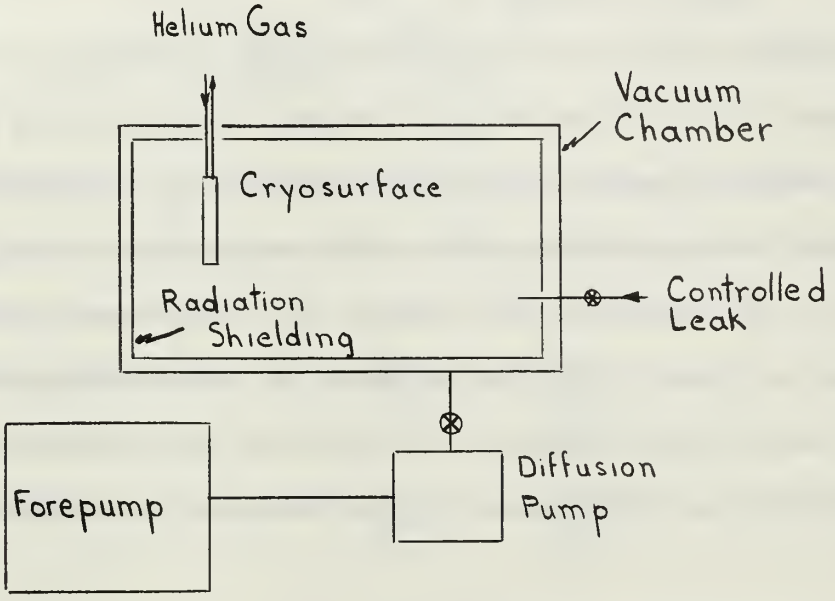

Fig. 2 System representation

gas and a variable leak valve is used to control the leakage rate of test gas into the chamber. Figure 3 is a representation of the plot of pressure versus time that would be obtained during an experimental run if only condensable gases were present.

At time t_1, the controlled leak is open to the chamber and the system is at equilibrium with both the diffusion pump and the cryosurface pumping. At time t_2, the system is isolated from the diffusion pump and

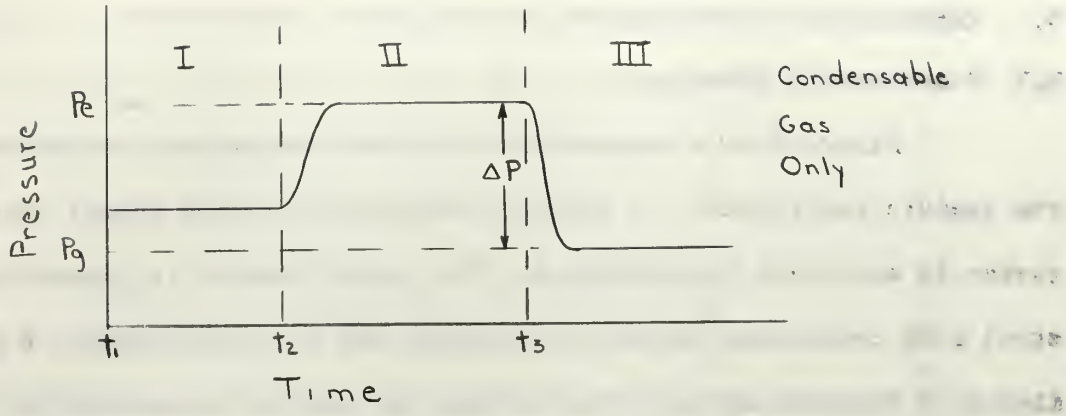

Fig. 3 Pressure vs. Time

the pressure rises until a new equilibrium pressure P_e is established. At time t_3, the inflow of gas is abruptly halted and the pressure drops until there is again an equilibrium pressure P_g with no flow into the chamber. Determination of the capture coefficient in this manner is known as the "pressure drop" method (10). Measurement of the ΔP depicted in Figure 3, the rate at which gas enters through the controlled leak, and the gas temperature are basic to the calculation of the capture coefficient as will be shown in the subsequent discussion.

5.2 Experimental equations.

Substitution of equation (4.5) into equation (4.15) gives an expression for the condensation coefficient.

$$f_g = \frac{Q_L}{\Delta P \, S_{th} \, A_s} \frac{T_g}{T_L} \qquad (5.1)$$

Where $\Delta P = P_e - P_g$. The use of the difference between the pressure with the leak on (P_e) and the pressure with the leak off (P_g) gives the condensation coefficient corrected for the vapor pressure of the condensed gas. Then, equation (4.15)

$$f = f_g\left(1 - \frac{P_g}{P_e}\right) \tag{4.15}$$

can be used to calculate the capture coefficient. If $P_g << P_e$, then the condensation coefficient and the capture coefficient are equal.

Equation (5.1) can be expressed in terms of measurable quantities by substitution of the expression for S_{th} (equation 3.14).

$$f_g = \frac{Q_L T_g}{\Delta P A_s T_L}\left(\frac{2\pi M}{R T_g}\right)^{1/2} \tag{5.2}$$

Through the use of the thermal transpiration equation, the measured pressure P_m can be obtained in terms of the gas temperatures and the chamber pressure.

With controlled leak: $$\frac{P_e}{\sqrt{T_g}} = \frac{P_{m1}}{\sqrt{T_m}}$$

Without controlled leak: $$\frac{P_g}{\sqrt{T_g}} = \frac{P_{m2}}{\sqrt{T_m}}$$

Therefore: $$\Delta P = (P_{m1} - P_{m2})\left(\frac{T_g}{T_m}\right)^{1/2}$$

and

$$f_g = \frac{Q_L}{A_s \Delta P_m T_L}\left(\frac{2\pi M T_m}{R}\right)^{1/2} \tag{5.3}$$

If the controlled leak and the pressure gage are at the same temperature, $T_m = T_L$, and

$$f_g = \frac{Q_L}{A_s \Delta P_m}\left(\frac{2\pi M}{R T_L}\right)^{1/2} \tag{5.4}$$

Through the use of a constant temperature pressure gage and the pressure drop method, thermal transpiration and vapor pressure effects are included in the expression for the condensation coefficient.

5.3 Experimental Measurements.

An examination of equation (5.4) reveals that the quantities that must be measured experimentally are: (a) the measured pressure drop, ΔP_m; (b) the temperature of the gas at the pressure gage, T_m and the temperature of the gas entering through the controlled leak, T_L; (c) the controlled leak throughput, Q_L, and (d) the area of the cryosurface, A_s. Each measurement involves assumptions that must be examined to ensure that this macroscopic approach is valid.

(a) Pressure Measurement.

In the foregoing analysis, it has been assumed that only one pure condensable gas was present in the chamber and that this same specie of gas was the only gas flowing through the controlled leak. In the actual situation this is not the case. Other condensable and non-condensable gases will be present due to (1) impurities in the gas admitted with the controlled leak, (2) inleakage of the local atmosphere through the chamber walls and the system seals and (3) outgassing from all the components of the system exposed to the vacuum. With these other gases present, the experimental pressure versus time curve will appear as shown in Figure 4.

The pressure in the chamber is the sum of the partial pressures of all the gases present in the system. Each condensable gas will have a different partial pressure because each gas has a different theoretical pumping speed. The pressure drop ΔP_m due to cryopumping is a result of

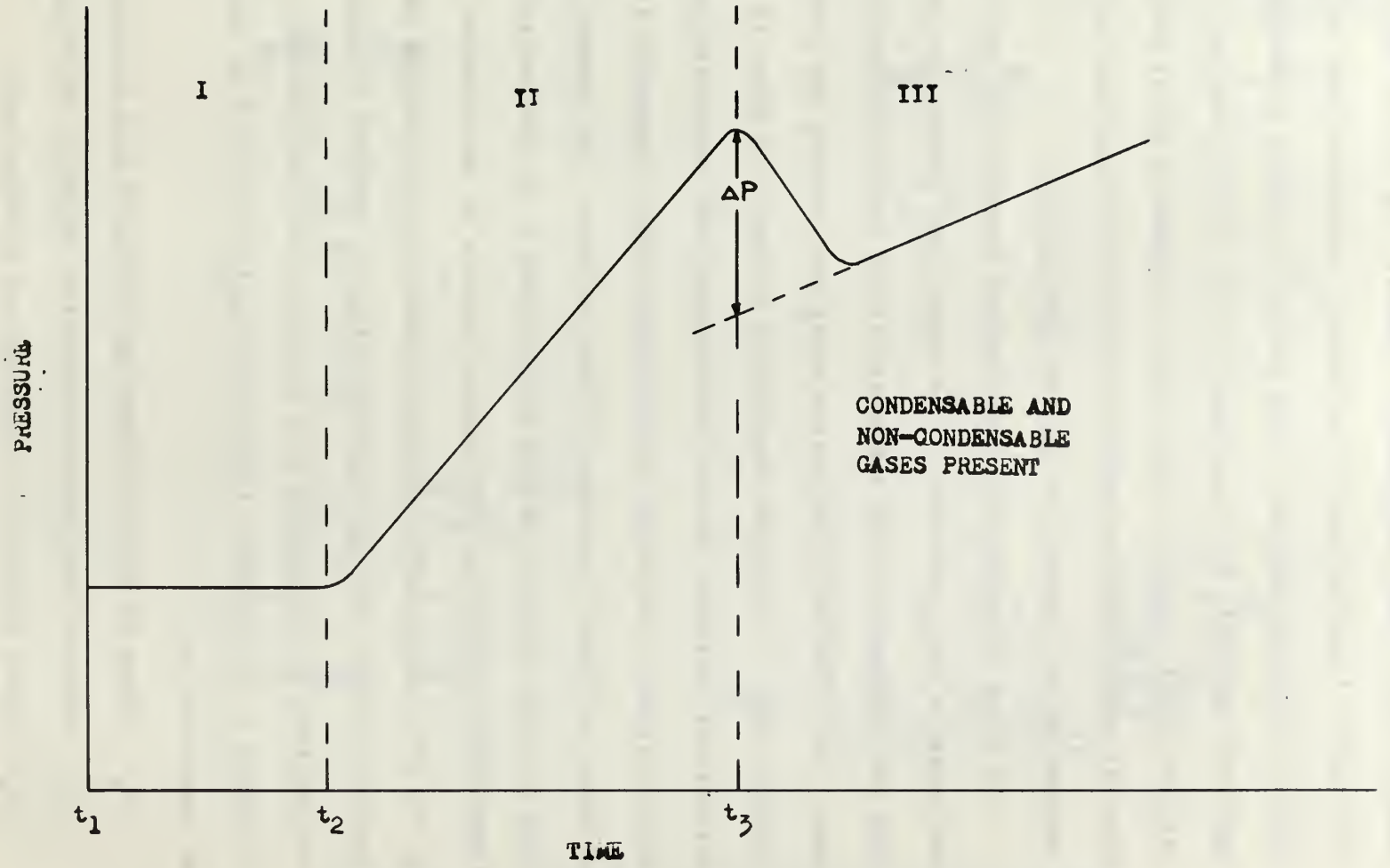

FIGURE 4. PRESSURE VS. TIME

the reduction in the partial pressures of all the condensable gases present. The measurement of the partial pressure of the test gas is possible with a mass spectrometer, however, one was not available for this work. A conventional Bayard-Alpert ionization gage, a nude Bayard-Alpert ionization gage and a cold cathode triggered discharge ionization gage were available for measurement of the system pressure. Therefore, only the total chamber pressure could be measured and it must be assumed that all other gases are present in quantities which are negligible when compared to the quantity of the test gas present.

In order to ensure that the measured pressure drop corresponds to the pressure drop predicted by the theory, the system must be analyzed from the standpoint of the molecular fluxes which occur during an experimental run. The following system model and analysis are from LT. L. C. Tedeschi (10). The system consists of a chamber in which is mounted a cylindrical radiation shield, two circular disk end shields and a gas addition system. The actual system is described in Appendix A. The model as shown in Figure 5 consists of three volumes. The chamber is divided into an inner volume V_i and an outer volume V_o by the radiation shielding. Conductance between the two volumes consists of two circular viewing ports in the end shields and a clearance between the end shields and the cylindrical shield. The gas addition volume V_a consists of tubing leading the gas from the controlled leak supply to the inner volume. Referring to Figure 5, the volumes, temperatures and molecular flow rates that must be considered are:

V_a - Volume of piping between gas injection stop valve and chamber

V_i - Volume of the chamber inside the radiation shielding

V_o - Volume between the shielding and the tank wall

T_o - Mean temperature of tank wall and the radiation shielding

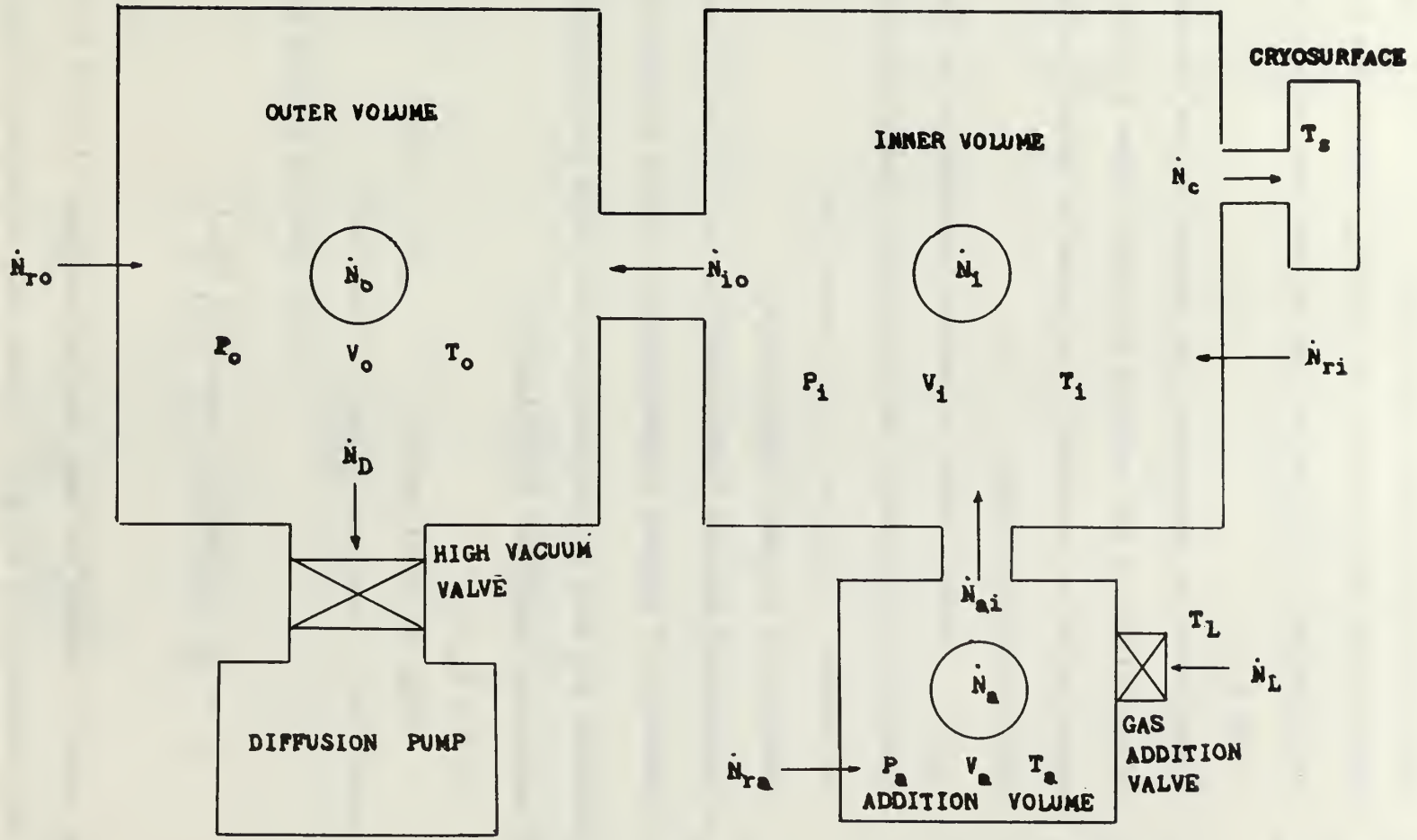

FIGURE 5. CONDENSABLE GAS MODEL FOR SYSTEM EQUATIONS

T_a - Temperature of the wall of the piping containing V_a

T_i - Temperature of the gas in V_i

T_L - Temperature of the gas admitted to V_a

$\dot{N}_L$ - Molecules/sec of controlled gas entering lines to the chamber

$\dot{N}_{ai}$ - Molecules/sec of controlled gas entering the inner volume V_i from V_a

$\dot{N}_c$ - Molecules/sec of condensable gas captured by the cryosurface

$\dot{N}_{io}$ - Molecules/sec of gas entering the outer volume V_o from V_i

$\dot{N}_D$ - Molecules/sec of condensable gas pumped by the diffusion pump and the cryogenic trap

$\dot{N}_{ra}$, $\dot{N}_{ri}$, $\dot{N}_{ro}$ - Molecules/sec of residual condensable gas from leakage into the chamber and outgassing of materials within the chamber

$\dot{N}_i$ - Summation of all gas fluxes into V_i

$\dot{N}_o$ - Summation of all gas fluxes into V_o

$\dot{N}_a$ - Summation of all gas fluxes into V_a

Expressions for each of the molecular flow rates are developed in terms of measurable quantities as follows:

(1) $\dot{N}_i$, $\dot{N}_o$, $\dot{N}_a$

From the ideal gas law

$$N = \frac{PVN_A}{RT}$$

$$\dot{N} = \frac{d}{dt}\left(\frac{PVN_A}{RT}\right) = \frac{1}{k}\frac{d}{dt}\left(\frac{PV}{T}\right)$$

The gases all occupy the same constant volumes. As will be seen later, the temperature in any given volume must be assumed constant.

Therefore,

$$\dot{N} = \frac{V}{kT}\dot{P}$$

and

$$\dot{N}_i = \frac{V_i}{kT_i}\dot{P}_i \tag{5.6}$$

$$\dot{N}_o = \frac{V_o}{kT_o}\dot{P}_o \tag{5.7}$$

$$\dot{N}_a = \frac{V_a}{kT_a}\dot{P}_a \tag{5.8}$$

(2) $\dot{N}_L$

The flow of controlled gas is

$$\dot{N}_L = \frac{1}{k}\frac{d}{dt}\left(\frac{P_L V_L}{T_L}\right)$$

where P_L and T_L are the pressure and temperature at the inlet to the gas addition piping and are constant so that

$$\dot{N}_L = \frac{P_L \dot{V}_L}{kT_L} = \frac{Q_L}{T_L} \tag{5.9}$$

(3) $\dot{N}_{ai}$, $\dot{N}_{io}$

From kinetic theory, the number of molecules incident on a surface per unit time is

$$\dot{N} = \frac{PA}{(2\pi mkT)^{1/2}}$$

Then

$$\dot{N}_{ai} = C_a\left(\frac{P_a}{\sqrt{T_a}} - \frac{P_i}{\sqrt{T_i}}\right) \tag{5.10}$$

where $$C_a = \frac{A_{ai}}{(2\pi mk)^{1/2}}$$

and A_{ai} is the area through which the gas flows as it travels from V_a to V_i. Similarly,

$$\dot{N}_{io} = C_i \left(\frac{P_i}{\sqrt{T_i}} - \frac{P_o}{\sqrt{T_o}} \right) \qquad (5.11)$$

(4) $\dot{N}_c$

The expression for the flow to the cryopanel is given by equation (4.11).

$$\dot{N}_c = \frac{A_s}{(2\pi mk)^{1/2}} \left(\frac{f_q P_i}{\sqrt{T_i}} - \frac{f_s P_s}{\sqrt{T_s}} \right) \qquad (4.11)$$

(5) $\dot{N}_D$

The volumetric pumping speed of a diffusion pump can be considered constant over the pressure range of interest here. The pumping speed curve for the pump employed in this system is shown in Figure 6. Since pressure change has no effect on the pumping speed,

$$\dot{N}_D = \frac{P}{kT} \dot{V}_D \qquad (5.12)$$

If, as in this system, the diffusion pump is used with a cryogenic trap, the limited conductance of the trap will reduce $\dot{V}_D$ and

$$\dot{N}_D = \left(\frac{\alpha \dot{V}_D}{kT_o} \right) P_o \qquad (5.13)$$

where α is an efficiency factor.

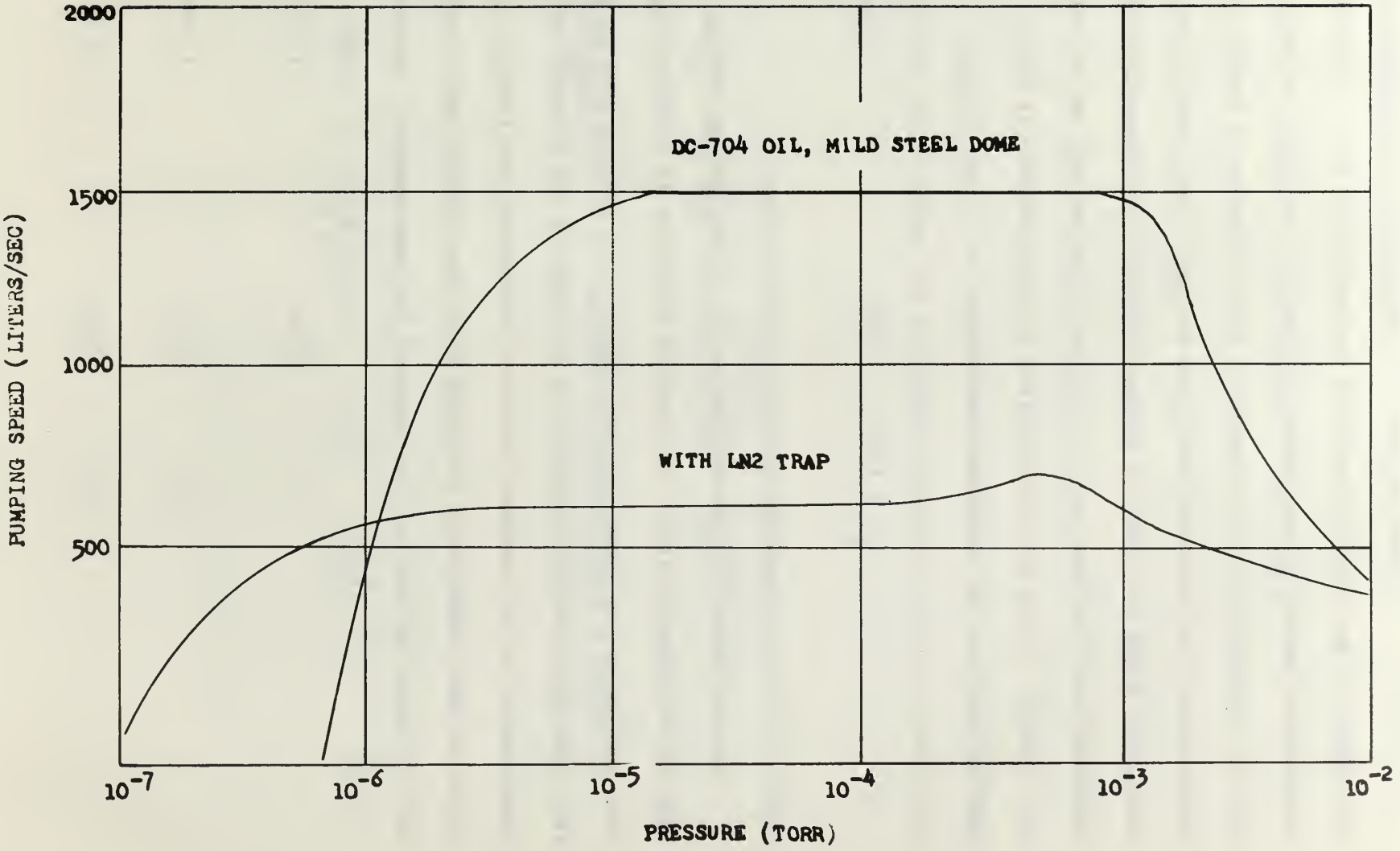

FIGURE 6. DIFFUSION PUMP CHARACTERISTICS

(6) $\dot{N}_r$

After exposure to atmospheric air for several hours, the amount of gas readily available for desorption from a surface at room temperature amounts to many molecular layers. Although the outgassing rate of a material is time dependent, after exposure to vacuum for considerable periods, the variation with time is small. For example, Dayton (11) shows that after ten hours of vacuum pumping, the outgassing rate for a stainless steel surface is 1×10^{-8} torr liter/sec-cm^2 and is decreasing very slowly. Since the time required for measurements is small, the outgassing rate will be considered constant.

$$\dot{N}_r = \frac{1}{k}\frac{d}{dt}\left(\frac{PV}{T}\right) = \frac{Q_r}{kT} \qquad (5.14)$$

where Q_r is the outgassing rate from a given surface.

The diffusion of a gas through metal is proportional to the square root of the pressure (12). The rate of diffusion is small and the pressure changes in the system are very small. The leakage rate is therefore considered constant and will be included in the term for outgassing. Measurements of the combined effects of outgassing and leakage in this system at room temperature indicated that these effects were constant over the short periods of time required for measurements. Therefore,

$$\dot{N}_{ra} = \frac{Q_{ra}}{kT_a} \qquad (5.15)$$

$$\dot{N}_{ri} = \frac{Q_{ri}}{kT_i} \qquad (5.16)$$

$$\dot{N}_{ro} = \frac{Q_{ro}}{kT_o} \qquad (5.17)$$

The following equations result from molecular rate balances on the three volumes shown in Figure 5.

$$\dot{N}_i = \dot{N}_{ri} + \dot{N}_{ai} - \dot{N}_c - \dot{N}_{io} \tag{5.18}$$

$$\dot{N}_o = \dot{N}_{io} + \dot{N}_{ro} - \dot{N}_D \tag{5.19}$$

$$\dot{N}_a = \dot{N}_L + \dot{N}_{ra} - \dot{N}_{ai} \tag{5.20}$$

Substitution of the expressions developed for the terms in these equations and solution for the rate of pressure change in each volume yields

$$\dot{P}_i = \frac{Q_{ri}}{V_i} + \left[\frac{f_s A_s T_i}{V_i}\left(\frac{k}{2\pi m T_s}\right)^{1/2}\right] P_s + \left[\frac{C_i}{V_i}\frac{kT_i}{\sqrt{T_o}}\right] P_o$$

$$+ \left[\frac{C_a k T_i}{V_i\sqrt{T_a}}\right] P_a - \left[\frac{C_a k\sqrt{T_i}}{V_i} + \frac{f_g A_s}{V_i}\left(\frac{kT_i}{2\pi m}\right)^{1/2} + \frac{C_i k\sqrt{T_i}}{V_i}\right] P_i \tag{5.21}$$

$$\dot{P}_o = \frac{Q_{ro}}{V_o} + \left[\frac{C_i k T_o}{V_o\sqrt{T_i}}\right] P_i - \left[\frac{\alpha \dot{V}_o}{V_o} + \frac{C_i k\sqrt{T_o}}{V_o}\right] P_o \tag{5.22}$$

$$\dot{P}_a = \frac{Q_{ra}}{V_a} + \frac{Q_i T_a}{V_a T_i} + \left[\frac{C_a K T_a}{V_a \sqrt{T_i}}\right] P_i - \left[\frac{C_a K \sqrt{T_a}}{V_a}\right] P_a \qquad (5.23)$$

By defining constants as in Table I, the equations above can be expressed as

$$\dot{P}_i = A + a_1 P_o + a_2 P_a - [a_3 + a_4 + a_5] P_i \qquad (5.24)$$

$$\dot{P}_o = B + a_6 P_i - [a_7 + a_8] P_o \qquad (5.25)$$

$$\dot{P}_a = C + D + a_9 P_i - a_{10} P_o \qquad (5.26)$$

These are the equations which describe the system. They have been solved on an analog computer by Tedeschi (10), and curves similar to that shown in Figure 3 have been obtained. Reference to Figure 3 and to equations (5.24), (5.25) and (5.26) yield the following solutions for steady state operations between times t_1 and t_2.

$$P_i(I) = \frac{a_{10}(a_7 + a_8)A + a_1 a_{10} B + a_2 (a_7 + a_8)(C + D)}{a_{10}(a_7 + a_8)(a_3 + a_4 + a_5) - a_1 a_6 a_{10} - a_2 a_9 (a_7 + a_8)} \qquad (5.27)$$

$$P_o(I) = \frac{B}{a_7 + a_8} + \frac{a_6}{a_7 + a_8} P_i(I) \qquad (5.28)$$

COEFFICIENT	EXPRESSION	COEFFICIENT	EXPRESSION
A	$\frac{Q_{ri}}{V_i} + \frac{f_s A_s T_h}{V_i}\sqrt{\frac{k}{2\pi m T_s}}$	a_4	$\frac{f_g}{V_i}\frac{A_s}{}\sqrt{\frac{kT_i}{2\pi m}}$
B	$\frac{Q_{ro}}{V_o}$	a_5	$\frac{C_i k\sqrt{T_i}}{V_i}$
C	$\frac{Q_{ra}}{V_a}$	a_6	$\frac{C_i k T_o}{V_o\sqrt{T_i}}$
D	$\frac{Q_L T_a}{V_a T_L}$	a_7	$\frac{\propto \dot{V}_D}{V_o}$
a_1	$\frac{C_i k T_i}{V_i\sqrt{T_o}}$	a_8	$\frac{C_i k\sqrt{T_o}}{V_o}$
a_2	$\frac{C_a k T_i}{V_i\sqrt{T_a}}$	a_9	$\frac{C_a k T_a}{V_a\sqrt{T_i}}$
a_3	$\frac{C_a k\sqrt{T_i}}{V_i}$	a_{10}	$\frac{C_a k\sqrt{T_a}}{V_a}$

TABLE I. COEFFICIENTS OF SYSTEM EQUATIONS

$$P_a(I) = \frac{C + D}{a_{10}} + \frac{a_9}{a_{10}} P_i(I) \qquad (5.29)$$

At time t_2, the diffusion pump is isolated from the system and therefore, $a_7 = \propto \dot{V}_D/V_o = 0$, and the equilibrium solutions are:

$$P_i(II) = \frac{a_1 a_6 + a_1 a_{10} E - a_2 a_8 (C - D)}{a_{10} a_8 (a_3 + a_4 + a_5) - a_1 a_6 a_{10} - a_2 a_8 a_9} \qquad (5.30)$$

$$P_o(II) = \frac{B}{a_8} + \frac{a_6}{a_8} P_i(II) \qquad (5.31)$$

$$P_a(II) = \frac{C + D}{a_{10}} + \frac{a_9}{a_{10}} P_i(II) \qquad (5.32)$$

At time t_3, the gas inflow is abruptly halted and therefore, $D = Q_L T_a / V_L T_L = 0$. The equilibrium solutions are:

$$P_i(III) = \frac{a_{10} a_8 + a_{10} B + a_2 a_8 C}{a_{10} a_8 (a_3 + a_4 + a_5) - a_1 a_6 a_{10} - a_2 a_8 a_9} \qquad (5.33)$$

$$P_o(III) = \frac{B}{a_8} + \frac{a_6}{a_8} P_i(III) \qquad (5.34)$$

$$P_a(III) = \frac{C}{a_{10}} + \frac{a_9}{a_{10}} P_i(III) \qquad (5.35)$$

The pressure drop in the inner volume is then

$$P_i(II) - P_i(III) = \frac{a_2 a_8 D}{a_8 a_{10}(a_3 + a_4 + a_5) - a_1 a_6 a_{10} - a_2 a_8 a_9} \qquad (5.36)$$

and substitution of the constants from Table I yields

$$P_i(II) - P_i(III) = \frac{Q_i T_i}{f_g A_e} \left(\frac{\gamma M}{T_i}\right)^{1/2}$$

or

$$f_g = \frac{Q_i}{A_e [P_i(II) - P_i(III)]} \left(\frac{\gamma M}{T_i}\right)^{1/2} \qquad (5.37)$$

This is the same expression as equation (5.2) when it is considered that:

T_i is the temperature of the gas in the inner volume and is therefore equal to T_g.

$P_i(II)$ is the equilibrium pressure with gas flow being admitted to the chamber and is therefore equal to P_e.

$P_i(III)$ is the equilibrium pressure with no gas flow to the chamber

and is therefore equal to P_g.

$$\Delta P = P_i(II) - P_i(III) = P_e - P_g$$

The experimentally observed pressure drop is therefore the same as that predicted by the theory providing the assumptions mentioned previously are valid and provided that the experimental pressure drop is measured in the inner volume V_i.

If the experimental pressure is measured in V_o, then the equations for the system predict

$$P_o(II) - P_o(III) = \frac{a_b}{a_s}\left[P_i(II) - P_i(III)\right] \qquad (5.28)$$

Substitution of the constants results in

$$P_o(II) - P_o(III) = \sqrt{\frac{T_o}{T_i}}\left[P_i(II) - P_i(III)\right] \qquad (5.29)$$

which indicates that an application of the thermal transpiration effect is all that is required to relate the pressure drop measured in the outer volume to the pressure drop measured in the inner volume. The measurement of the pressure drop in the outer volume however, may not accurately reflect the rate of incidence of molecules on the cryosurface. If the conductance between the inner and outer volumes is not large, this conductance may have a significant effect on the measurement of the capture coefficient.

If the two volumes are considered connected by a conductance of area β, with the gas inflow into V_i as shown in Figure 7, the effect of the conductance may be determined in the following manner.

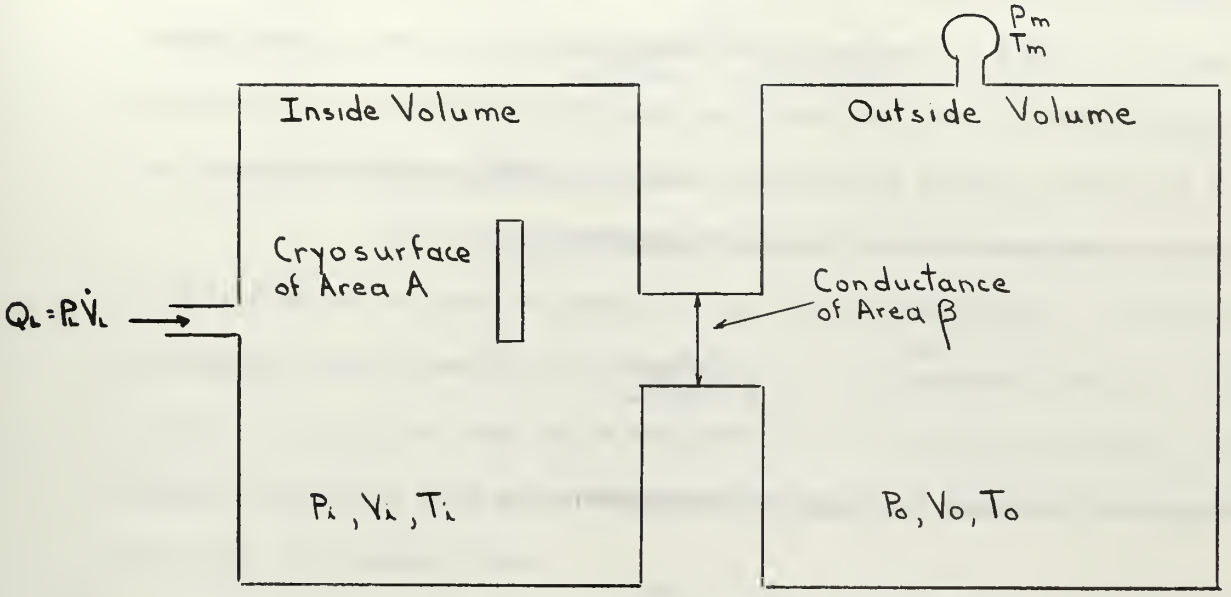

Fig. 7 Conductance Effects

At steady state,

$$\frac{N_A P_L \dot{V}_L}{R T_L} = \frac{f A P_i}{(2\pi m k T_i)^{1/2}} \qquad (5.40)$$

and

$$\frac{\beta P_o}{(2\pi m k T_o)^{1/2}} - \frac{\beta P_i}{(2\pi m k T_i)^{1/2}} = \frac{f A P_i}{(2\pi m k T_i)^{1/2}} \qquad (5.41)$$

Solution of both equations for P_i and a subtraction yields,

$$P_o - \frac{N_A P_L \dot{V}_L}{\beta R T_L} (2\pi m k T_o)^{1/2} = \frac{N_A P_L \dot{V}_L}{A f R T_L} (2\pi m k T_o)^{1/2} \qquad (5.42)$$

P_o can be eliminated by using thermal transpiration and if $T_m = T_L$, then

$$P_m S_{th} - \frac{P_L \dot{V}_L}{\beta} = \frac{P_L \dot{V}_L}{A f} \qquad (5.43)$$

and solving for the capture coefficient

$$f = \frac{\beta Q_L}{\beta A P_m S_{th} - A P_L V_L} \tag{5.44}$$

If f* is the capture coefficient measured without any conductance effects, then equation (4.5) can be expressed as

$$f^* = \frac{Q_L}{A S_{th} P_m} \tag{5.45}$$

The ratio of these two capture coefficients is

$$\frac{f^*}{f} = \frac{\beta - f^* A}{\beta} \tag{5.46}$$

so that unless the product of the cryosurface area and the capture coefficient without conductance (f*) is small compared to the conductance area, the effect cannot be ignored. In order to eliminate the effect of limited conductance, it is desirable to measure the pressure in the volume containing the cryosurface.

(b) Gas temperature.

In order for the gas within the chamber to have a defined temperature, it must be assumed that the molecular velocities are distributed in accordance with the Maxwell-Boltzman velocity distribution function. Since the pressure is low enough so that the mean free path of the molecules is large compared with the dimensions of the system, intermolecular collisions are rare and collisons of the molecules with the chamber walls predominate. Under this condition, gas molecules will assume the local temperature of the wall. In order for the Maxwell-Boltzman distribution to have meaning, the ratio of wall surface area to

the cryosurface area must be large, the temperature of the walls must be uniform and diffuse flow must be assured. If there is directed flow and/or non-uniform wall temperatures, the gas may no longer have the statistical distribution required and there will be no defined temperature.

(c) Flow measurement.

The metered flow of test gas into the chamber must be accurately known in order to compute the capture coefficient. Flow measurement was accomplished by measuring the rate of pressure rise in a known volume. A variable leak valve was used to set the flow rate and a Bayard-Alpert ionization gage or a thermocouple pressure gage used to measure the rate of pressure rise.

In all cases, high purity research gas was employed to reduce the effects of other condensable and non-condensable gases in the system. The flow was deflected upon entry to the system containing the cryosurface to insure diffuse flow.

(d) Area Measurement.

The easiest way to ensure an accurate determination of the area of the cryosurface is to use a simple spherical geometry. This system however, employs a commercially produced cryosurface consisting of one flat side while the other side is embossed to provide channels for circulating the cryogenic fluid. A template was made of the embossed side of the cryosurface in order to make an accurate determination of the area of the cryosurface.

Because of the way in which this system is built, installation of vacuum insulated transfer lines within the vacuum would require a major redesign of the system. Therefore radiation shielding was provided around the line to reduce the heat load on the transfer lines. A

measurement of the temperature of the shielding while cold gaseous helium at approximately 20°K was flowing to the cryosurface revealed that the transfer lines need not be considered as part of the cryosurface area.

6. Experimental Results

Condensation coefficients for 300°K nitrogen are presented in tabular form in Table II. The condensation coefficient is plotted as a function of the gas throughput in Figure 8, and as a function of the pressure drop in Figure 9. The pressure gage within the volume containing the cryosurface was inoperative during the collection of data, therefore the pressure drop reported in Table II was measured in the outer volume of the chamber at the tank wall. Accordingly, the condensation coefficients tabulated in Table II have been corrected for conductance effects between the two volumes.

Table II Results of Cryopumping Nitrogen at 300°K

$Q_L \times 10^2$ (torr liters sec^{-1})	$\Delta P \times 10^6$ (torr)	$T_s \pm 3°K$ (°K)	f_g
0.061	0.0167	25.0	0.67
0.165	0.0394	25.0	0.71
0.222	0.0586	25.0	0.68
0.226	0.0680	25.0	0.62
0.489	0.135	25.0	0.66
0.644	0.174	25.0	0.67
0.745	0.210	25.0	0.65
0.980	0.284	25.0	0.64
2.12	0.554	25.0	0.69
2.44	0.715	25.0	0.63
2.52	0.705	12.0	0.66
3.04	0.880	25.0	0.64
4.05	1.11	25.0	0.67
4.20	1.21	25.0	0.64
4.30	1.16	25.0	0.69
4.67	1.36	25.0	0.64
6.00	2.00	25.0	0.58
6.08	2.00	25.0	0.58
7.70	2.39	12.0	0.61
9.20	3.61	25.0	0.51
9.22	3.28	12.0	0.55
10.4	3.81	25.0	0.54
11.3	4.19	12.0	0.53
11.5	4.38	12.0	0.52
13.1	5.53	25.0	0.48

Table II Results of Cryopumping Nitrogen (Cont'd)

$Q_L \times 10^2$ (torr liters sec^{-1})	$\Delta P \times 10^6$ (torr)	$T_s \pm 3°K$ (°K)	f_g
13.4	5.69	12.0	0.48
15.8	6.93	25.0	0.47
16.2	7.27	25.0	0.46
16.8	8.62	25.0	0.41
21.6	9.48	25.0	0.44
22.0	11.0	25.0	0.42
27.2	17.3	12.0	0.34
42.5	34.6	25.0	0.28
43.5	51.5	25.0	0.20
46.5	55.3	25.0	0.20
50.5	59.6	25.0	0.20
56.5	59.9	12.0	0.22
68.5	96.0	25.0	0.17
82.0	195.0	25.0	0.11
86.0	168.0	25.0	0.12
87.0	244.0	25.0	0.10
87.0	217.0	25.0	0.10

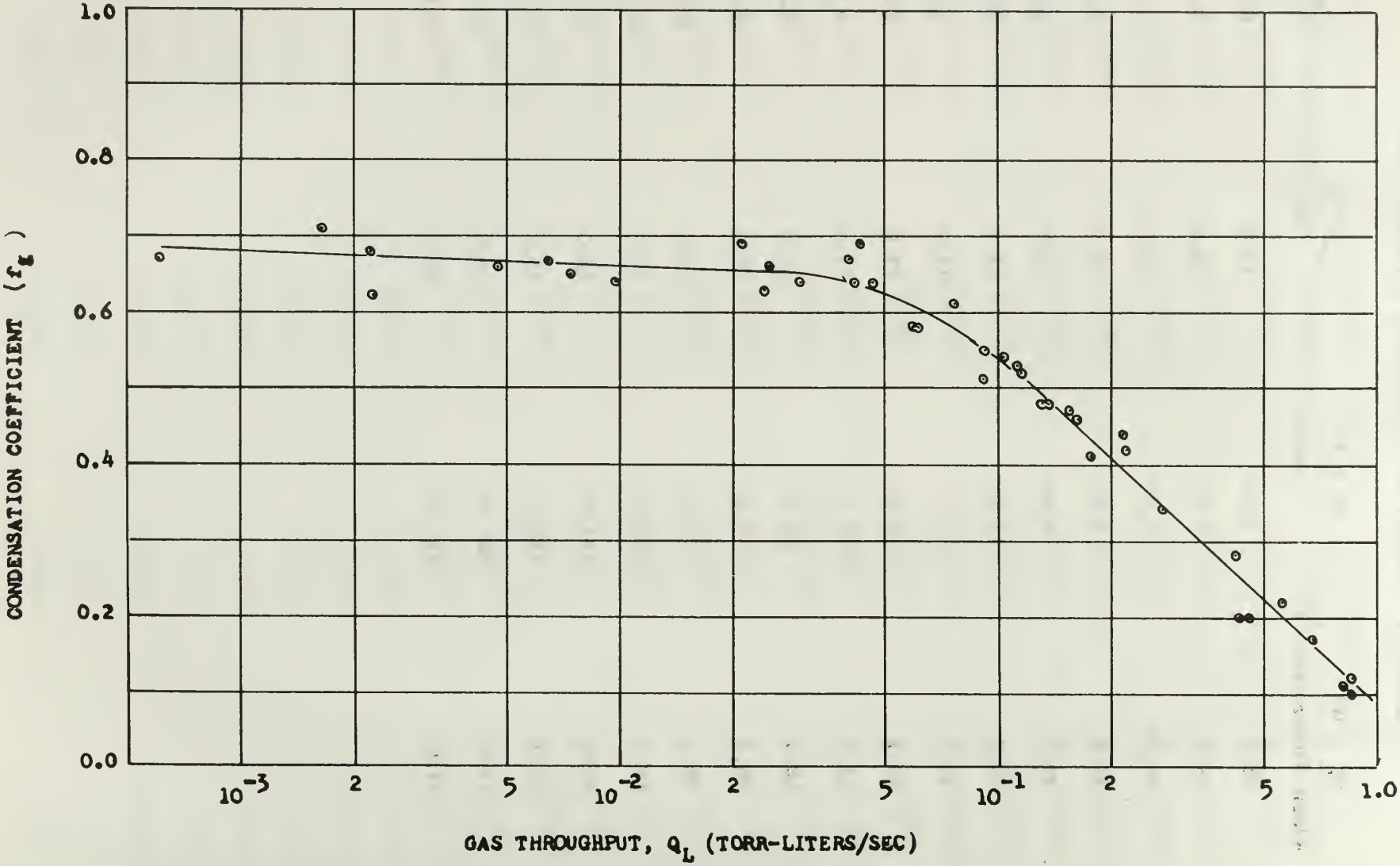

FIGURE 8. CONDENSATION COEFFICIENTS FOR 300°K NITROGEN

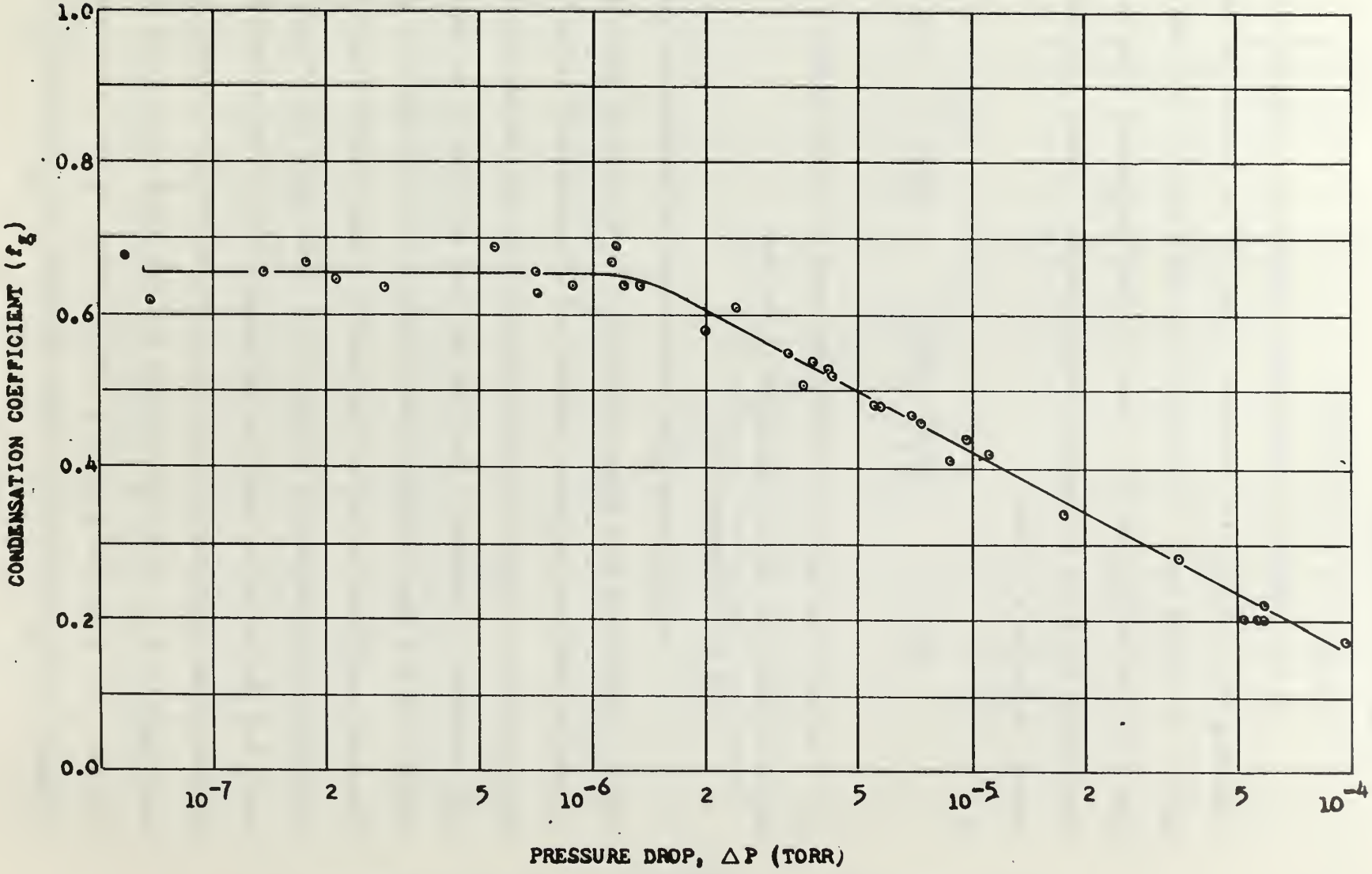

FIGURE 9. CONDENSATION COEFFICIENTS FOR 300°K NITROGEN

7. Discussion of Results

7.1 Analysis of Uncertainties

The reliability of the results obtained can be ascertained by examining the uncertainties involved in each of the fundamental measurements. The method used in estimating the uncertainty of the result is from Kline and McClintock (13). Each variable is assumed to be normally distributed and since the capture coefficient is a linear function of several variables v_i, then

$$\frac{\Delta f}{f} = \left[\left(\frac{\Delta V_1}{V_1}\right)^2 + \left(\frac{\Delta V_2}{V_2}\right)^2 + \cdots \left(\frac{\Delta V_n}{V_n}\right)^2 \right]^{1/2} \quad (7.1)$$

The variables and the uncertainties associated with them are tabulated in Table III and are explained as follows:

(a) Gas throughput, Q_L.

The gas throughput was measured by plotting the pressure rise $\dot{P}_L$ versus time in a known volume, V_L. An ionization gage was used to measure pressure rise when possible and a thermocouple pressure gage was used when the rate of pressure rise was too fast for the ionization gage recorder to response. The flow was then switched to the main chamber and the same throughput was assumed to flow to the main chamber. The uncertainty here is due to the possible change in the nature of the flow from free molecular to viscous flow. When using the thermocouple gage, X-Y plotter graph paper was calibrated for various pressures indicated on the meter and the resulting plot on non-linear coordinates was transferred to linear coordinates and the slope measured at 60 microns. The slope was generally linear between 40 and 80 microns. A sample of the linear plot is shown in Figure 10. This plot is typical

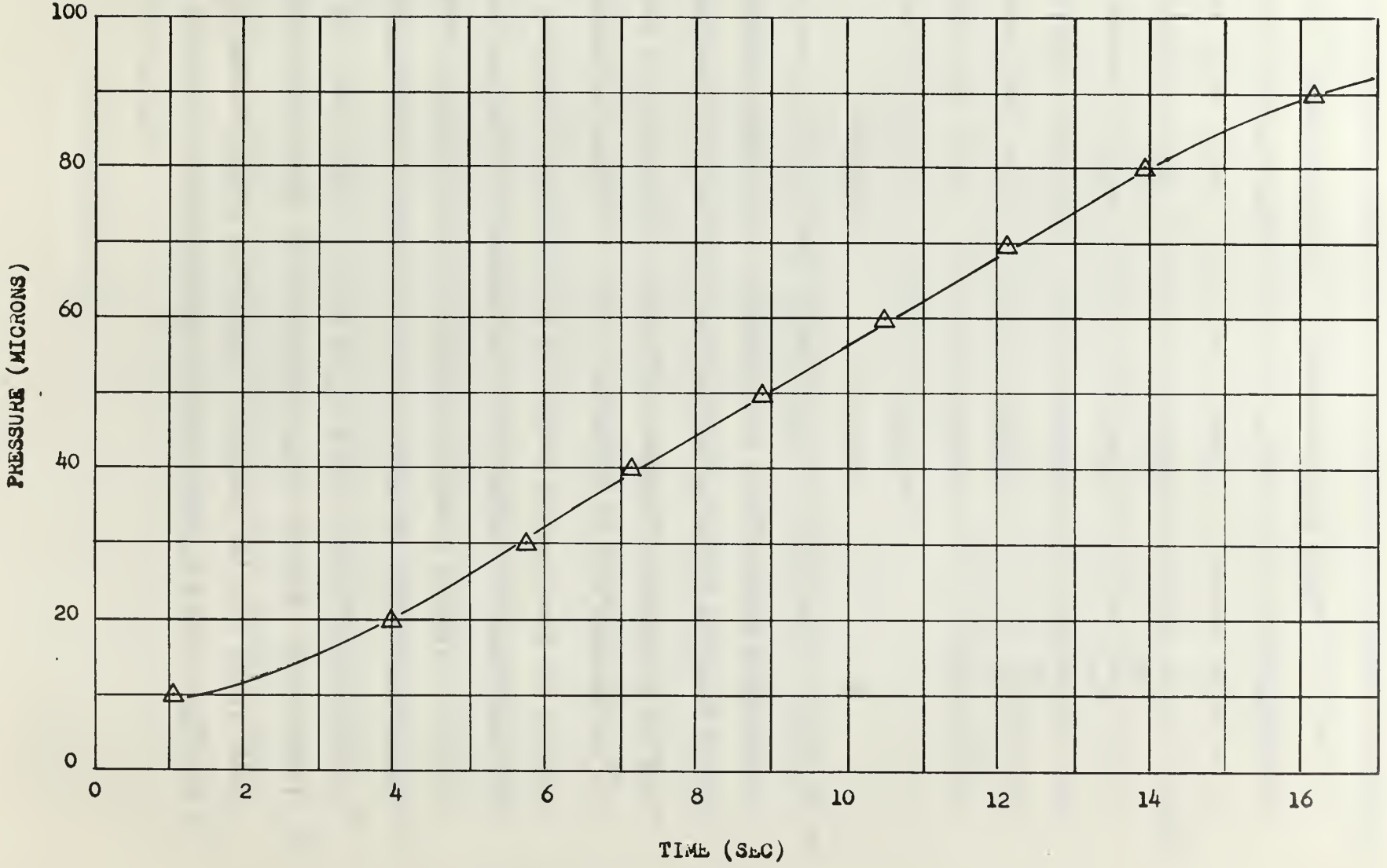

FIGURE 10. SAMPLE FLOW MEASUREMENT

of the way every flow measured plotted onto linear coordinates. There is an initial curvature, a linear portion between approximately 40 and 80 microns, and then another curvature at higher pressures. The initial

Table III Uncertainties in Measured Values

Quantity	Value	Uncertainty	Fraction
T_L	300°K	3°K	0.01
T_g	300°K	3°K	0.01
A_s	3300 cm^2	50 cm^2	0.015
V_L	4350 cm^3	30 cm^3	0.007
$\dot{P}_L$	Variable	---	0.10
ΔP	Variable	---	0.02
P	Variable	---	0.02
ρ	7780 cm^2	500 cm^2	0.064

curvature is attributed to gage response time and to the fact that the thermocouple pressure gage is not accurate below about 40 microns. The final curvature is due to the fact that the flow is in the viscous region and the throughput is proportional to $(P_o^2 - P_L^2)$ where P_o is the pressure on the upstream side of the variable leak. The question remains as to whether the flow measured between 40 to 80 microns is viscous, molecular or transitional. A calculation in accordance with the equations in Van Atta (14) yields a transition pressure (P_t) for nitrogen at 300°K in quarter-inch tubing of approximately 110 microns. The transition region conventionally extends from $0.1P_t$ to $10P_t$ or in this case from 1.1 to 1100 microns. This is in good agreement with Dawson's definition (6) which states that the transition region lies between Knudsen numbers of 0.01 and 10. The Knudsen number is the ratio of the mean free path to a

characteristic dimension of the system. This definition yields a transition region extending from 1.5 microns to 1500 microns. Therefore, the slope as measured between 40 and 80 microns in Figure 10 lies in the lower end of the transition region. In order to determine whether viscous forces had any significant effect in this area a comparison of the pressure rise as determined by the thermocouple gage and the pressure rise determined by the ionization gage was made at flow rates where it was possible to do. These checks indicated that the thermocouple gage indicated flows that were high by an average of 10%. It was therefore concluded that viscous forces played a minor role at the pressures in question and that the uncertainty in $\dot{P}_L$ is 10%.

(b) Temperatures.

The thermocouples used were calibrated with the use of an NBS computer program (15). Voltages from different junctions were reproducible within 20 microvolts for LN2-ICE junction giving an accuracy of about 1°K. Some difficulty however, was experienced with stray currents and it is considered that the accuracy is no better than $\pm$ 3°K.

(c) Pressure and Pressure Drop.

The accuracy of the Bayard-Alpert gage is quoted by the manufacturer as 2% when measuring the pressure of nitrogen. There is however, another uncertainty associated with the measurement of the pressure drop, ΔP. This is due to the slightly non-linear response of the ionization gage to the actual pressure. The recorder used to measure ΔP has a linear response. A maximum difference of 0.2 divisions over a measurement of 10 divisions was observed between the gage output and the recorder response.

(d) Cryosurface Area.

The area of the cryosurface is difficult to measure because of the embossing on one side. A template was made to fit the surface and then flattened and its area measured. It is estimated that this measurement is within 50 cm^2 of the actual area.

(e) Conductance Area.

The pressure gage located within the shielding with the cryosurface was inoperative during the time that data was taken, hence the effect of the conductance between the inner and outer volumes must be taken into account. This area consists of two holes in the end shields for viewing and spaces between the center and end shields. Measurement of all these areas was accomplished while the chamber was open, however because of the way the system is built, the center shield is inclined at an angle to the end shields. An average of several measurements was used to compute the area.

Substituting the values in Table III into equation (7.1) yields

$$\frac{\Delta f_g}{f_g} = 0.124 \qquad (7.2)$$

The uncertainty for the capture coefficient is not estimated since the partial pressure of the test gas could not be measured. If the assumption is made that the vapor pressure of the test gas is much less than the chamber equilibrium pressure obtained with gas flow on, then

$$\frac{\Delta f}{f} = 0.124 \qquad (7.3)$$

7.2 Comparison with Published Data

Table IV lists the published results for the capture coefficient of 300°K nitrogen.

Table IV Comparative Data on Capture Coefficients

Cryosurface Temperature in °K	Throughput in torr liters per second	Capture Coefficient	Reference
10.0	Not reported	0.65	6
12.5	Not reported	0.63	6
15.0	Not reported	0.62	6
17.5	Not reported	0.61	6
20.0	Not reported	0.60	6
22.5	Not reported	0.60	6
25.0	Not reported	0.60	6
32.5	0.0092	0.50	10
32.5	0.004	0.71	10
32.5	0.00296	0.72	10
32.5	0.004	0.67	10

8. Conclusions.

The results obtained for gas throughputs of less than 5×10^{-2} torr liters/sec agree well with the published data. For flows higher than this value, the capture coefficient decreases rapidly. Results for carbon dioxide obtained by Tedeschi (10) also indicate a decrease in the capture coefficient with increasing flow rate, but the abrupt break visible in Figures 8 and 9 is not indicated. Capture coefficients for nitrogen reported in the literature list only the variation with gas and/or cryosurface temperature.

Since the theoretical pumping speed remains constant with constant gas temperature and cryosurface area, the results indicate that the actual pumping speed decreases after a certain gas load is placed upon the system. Initially, high flow rate measurements were made after an appreciable quantity of condensate had accumulated on the panel. It was thought that perhaps the temperature of the condensate surface had increased enough to decrease the capture coefficient. Subsequent measurements at high flow rates with a bare cryopanel refuted this contention since the capture coefficients at high flow rates with and without a condensate layer were almost identical. The increase in gas load causes an increase in the system equilibrium pressure and hence a decrease in the mean free path of the gas molecules. The break in the curves of Figures 8 and 9 occurs at a chamber equilibrium pressure of approximately 2×10^{-6} torr. If the transition region is taken to begin at a Knudsen number of 10, then it begins at a pressure of approximately 10^{-5} torr for this system. Hence free molecular flow conditions still existed at the pressure at which the actual pumping speed begins to decrease. Dawson (6) indicates that pumping speed will increase upon entry into the transition region. Therefore, departure from free molecular flow is not believed to be the

cause of the decrease in pumping speed that was observed.

It would appear that the decrease in pumping speed may be caused by the increasing heat load placed on the panel by the higher flow rates. Instrumentation of the system to allow a measurement of the heat energy absorbed by the circulating helium gas and the heat load imposed on the panel at various gas throughputs should help in resolving the effect of high flow rates on the capture coefficient.

It is recommended that further work be done in this area in an effort to verify this decrease in experimental pumping speed with high gas loads.

BIBLIOGRAPHY

1. Roberts, R. W. and St. Pierre, L. E., Science, Vol.147, 26 March 1965.

2. Alpert, D., Review of Scientific Instruments, Vol.22, 1951.

3. Wang, E. S. J., Collins, J. A. Jr. and Haygood, J. D., "General Cryopumping Study", Advances in Cryogenic Engineering, Vol.7, Plenum Press 1962.

4. Chaun, R. L., and Wallace, D., "Present Status of Cryopumping", USEC Memorandum No. 1, November, 1960.

5. Brown, R. F., and Wang, E. S. J., "Capture Coefficients of Gases at 77°K", Advances in Cryogenic Engineering, Vol. 10, Plenum Press, 1963.

6. Dawson, J. P., and Haygood, J. D., "Cryopumping", Cryogenics, Vol. 5, April 1965.

7. Dawson, J. P. and Haygood, J. D., "Temperature Effects on the Capture Coefficient of Carbon Dioxide", AEDC-TDR-63-251, January 1964.

8. Dawson, J. P., "Temperature Effects on the Capture Coefficient of Six Common Gases", AEDC-TDR-64-84, May 1964.

9. Rogers, K. W., "Experimental Investigations of Solid Nitrogen Formed by Cryopumping", NASA CR-553, August 1966.

10. Tedeschi, L. C., "Capture Coefficients of Carbon Dioxide and Nitrogen Gas on a Cryogenic Cooled Surface", Thesis, Naval Postgraduate School, 1966.

11. Dayton, B. B., "Outgassing Rate of Contaminated Metal Surfaces", 1961 Vacuum Symposium Transactions, Permagon Press Inc., 1962.

12. Scott, R. B., Cryogenic Engineering, D. Van Nostrand Company Inc., New Jersey, 1959.

13. Kline, S. J., and McClintock, F. A., "Uncertainties in Single-Sample Experiments", Mechanical Engineering, January, 1953.

14. Van Atta, C. M., Vacuum Science and Engineering, McGraw Hill Inc., 1965.

15. Powell, R. L. and Sparks, L. L., "Available Low Temperature Thermocouple Information and Services", NBS Report 8750, February, 1965.

16. Albero, C. M., "Design and Development of a Cryogenic Pumping Evaluation Facility", Thesis, Naval Postgraduate School, 1965.

17. LaChance, G. M., "The Theory and Construction of a Liquid Helium Cryopump", Thesis, Naval Postgraduate School, 1964.

18. Levenson, L. L., Milleron, N., and Davis, D. H., "Optimization of Molecular Flow Conductance", 1960 Vacuum Symposium Transactions, Permagon Press, 1961.

19. Landfors, A. A., and Hablanian, M. H., "Diffusion Pump Speed Measurements at Very Low Pressure", 1958 Vacuum Symposium Transactions, Permagon Press, 1959.

20. Kennard, E. H., Kinetic Theory of Gases, McGraw Hill Inc., 1938.

APPENDIX A

General Description of the System

The system used for the measurement of the capture coefficient has been built and modified by previous investigators (10, 16, 17). Schematics and photographs are included as Figure 11, 12, 13 and 14. A brief description of the system follows:

(a) Main Vacuum Chamber.

The chamber is a modified forty inch diameter vacuum furnace manufactured by NRC. The volume of the chamber is 994 liters.

(b) Pumping System.

The pumping system consists of an NRC 100 CFM single stage mechanical forepump with a blank off pressure of 10 to 15 microns and a six inch, four stage, fractionating diffusion pump with a blank off pressure of approximately 10^{-7} torr when Dow Corning 704 diffusion pump fluid is used.

(c) Radiation Shielding.

The radiation shield is a 33 inch diameter, 36 inch long, type 304 stainless cylindrical shell plus two 36 inch diameter end shields. All shields are single embossed and are manufactured by Dean Products Inc. The volumetric capacity of the shielding is about 33 liters of liquid nitrogen with approximately 65 liters required for initial cooldown and fill.

(d) Cryopanel.

The cryopanel is constructed of two 12" x 20" type 304 stainless steel sheets. One sheet is embossed to provide channels for the cooling fluid. The sheets are welded together at the edges and the panel is electropolished.

(e) Instrumentation.

(1) Pressure Measurement.

In the pressure range above 10^{-3} torr, Vacuum Electronics Corporation thermocouple pressure gages are used to measure pressure. In the range below 10^{-3} torr, a conventional Bayard-Alpert ionization gage and a General Electric cold cathode triggered discharge gage are used. These gages are mounted on the chamber wall and measure the pressure in the chamber between the wall and the radiation shielding. A nude Bayard-Alpert gage is mounted within the radiation shielding.

(2) Temperature Measurement.

Teflon-insulated, 24 gage copper constantan thermocouples are used to measure the shield and cryopanel temperatures. Figure 15 is a schematic of the location of the thermocouples. A National Bureau of Standards computer program (15) was used to calibrate the thermocouples. The output of the thermocouples is fed through a differential amplifier to a digital voltmeter-printer combination.

(3) Controls.

All necessary electrical controls are located in a desk top panel. The system is arranged so that a high pressure in the chamber or a power failure will secure the power to the diffusion pump and isolate the chamber by shutting the high vacuum and foreline valves. Power to the diffusion pump is also secured in the event of high diffusion pump temperature.

Modifications made to the system this year include:

(1) Replacement of the silicone O-ring on the access door with an O-ring of Viton A.

(2) Installation of the General Electric triggered discharge gage.

(3) Modification of the safety circuits so that the diffusion pump would be shut down and the foreline and high vacuum valves would be shut in the event of either an overpressure or a power failure.

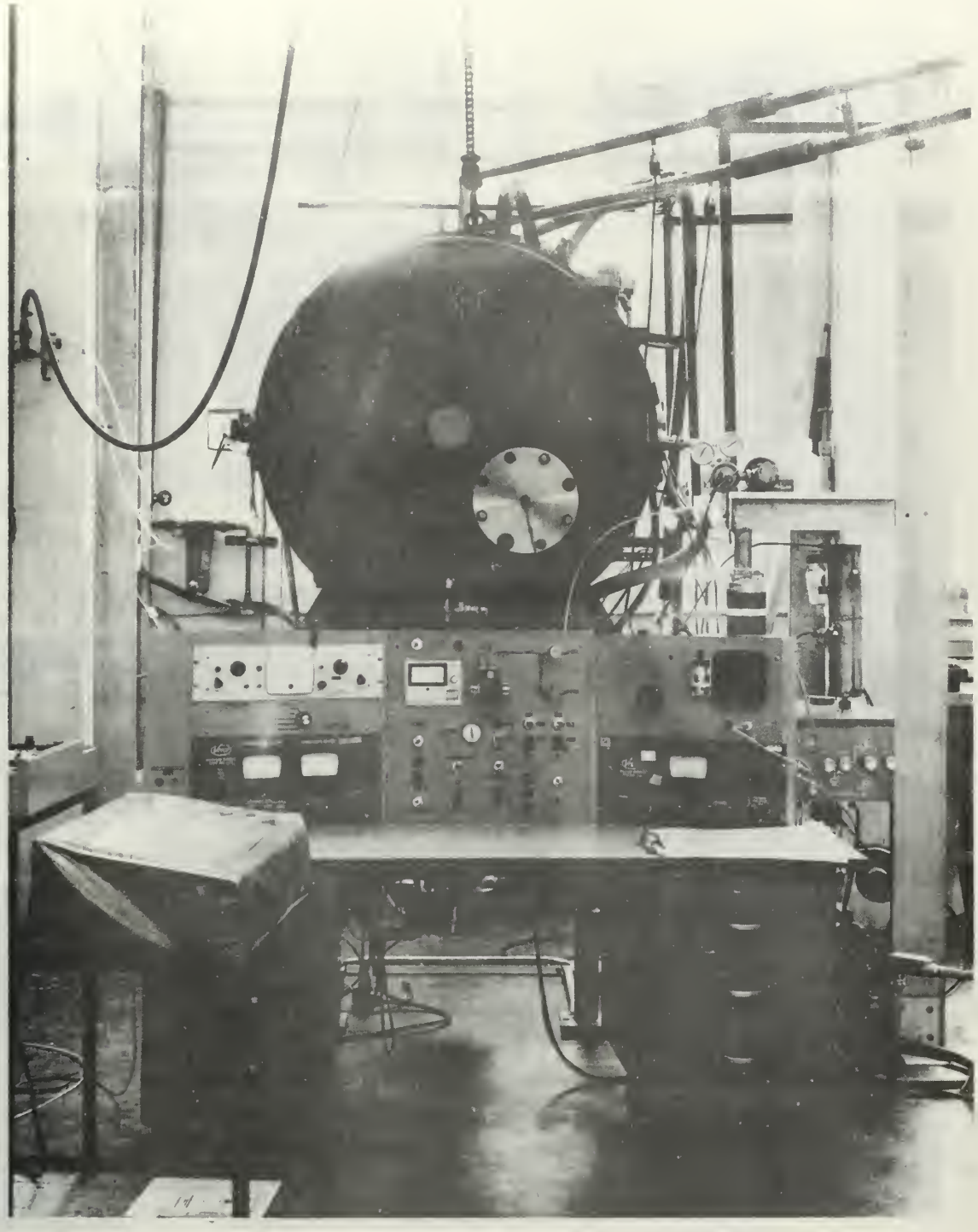

FIGURE 11. FRONT VIEW OF SYSTEM

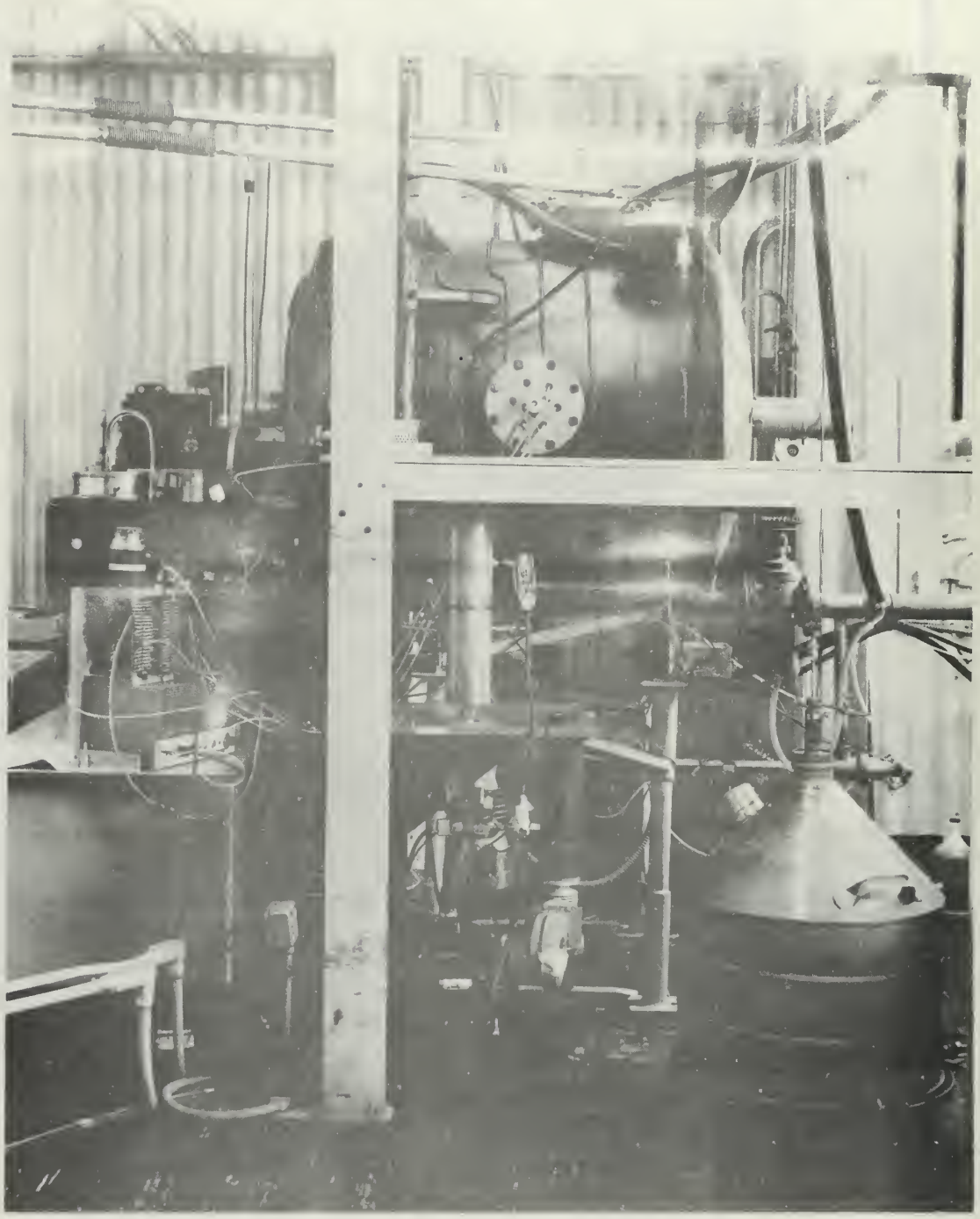

FIGURE 12. SIDE VIEW OF SYSTEM

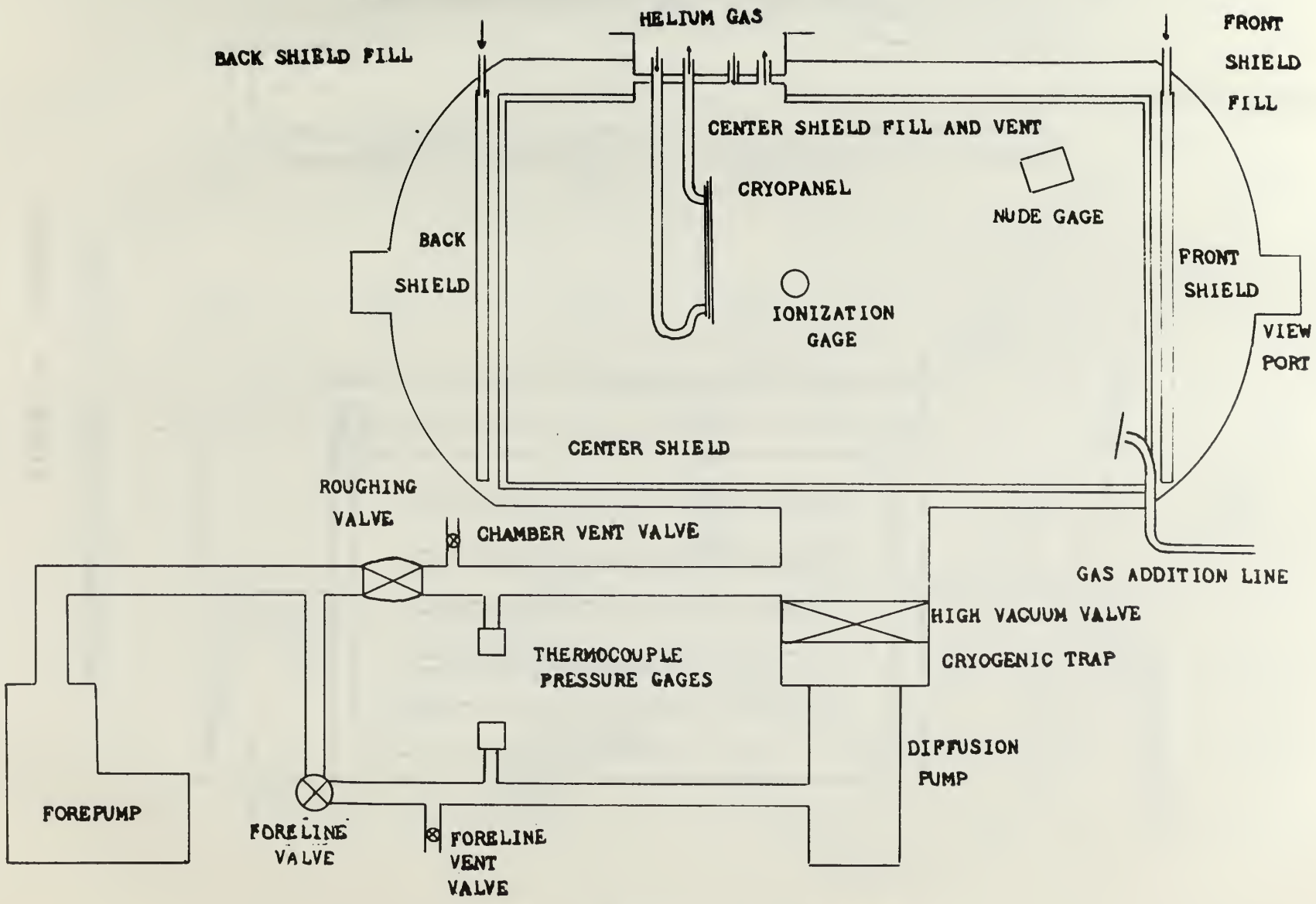

FIGURE 13. SCHEMATIC OF THE SYSTEM

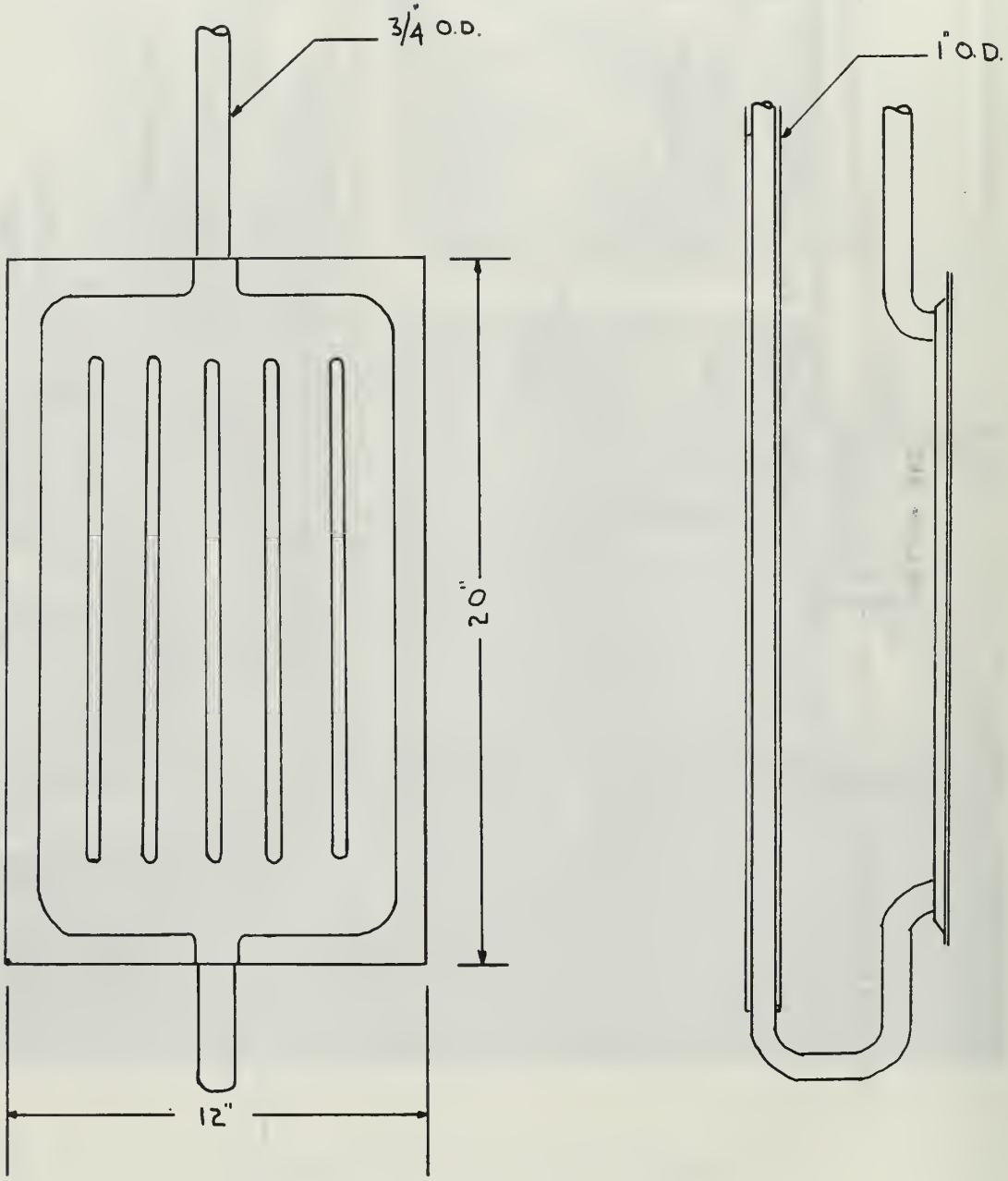

FIGURE 14. CRYOPANEL

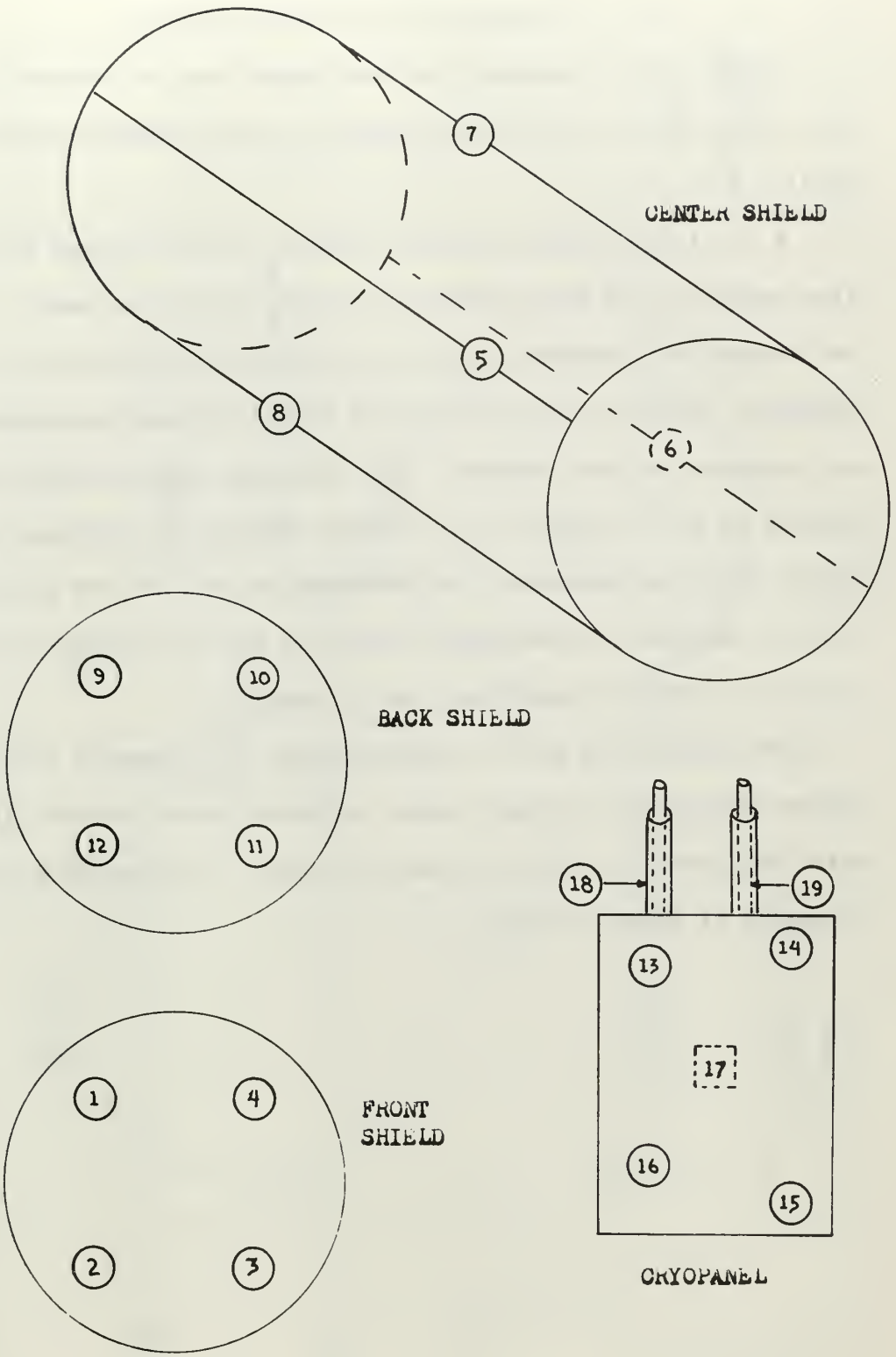

FIGURE 15. LOCATION OF THERMOCOUPLES

APPENDIX B

Cryogenic Fluid Transfer System

Figure 16 is a schematic of the system used to transfer liquid nitrogen to the shields and diffusion pump trap and gaseous helium to the cryopanel.

A 172 liter dewar was used to supply liquid nitrogen to the diffusion pump trap and the radiation shielding within the tank. The dewar was pressurized to approximately 8 psig with helium during the initial transfer. Later on, boil off of the liquid nitrogen maintained sufficient pressure for the transfer. The shielding requires approximately 35 minutes to fill. Figure 17 is a curve showing the cooldown time for the center shield as measured by a thermocouple near the top of the shield. Once the shields are partially filled, the rate of filling must be reduced in order to prevent geysering from the vents.

The cold helium gas is transferred to the cryopanel from an A.D. Little helium refrigerator through vacuum jacketed helium transfer lines. The heat loss from each line is about 0.45 watts. The cooldown curve for the cryopanel is shown in Figure 17.

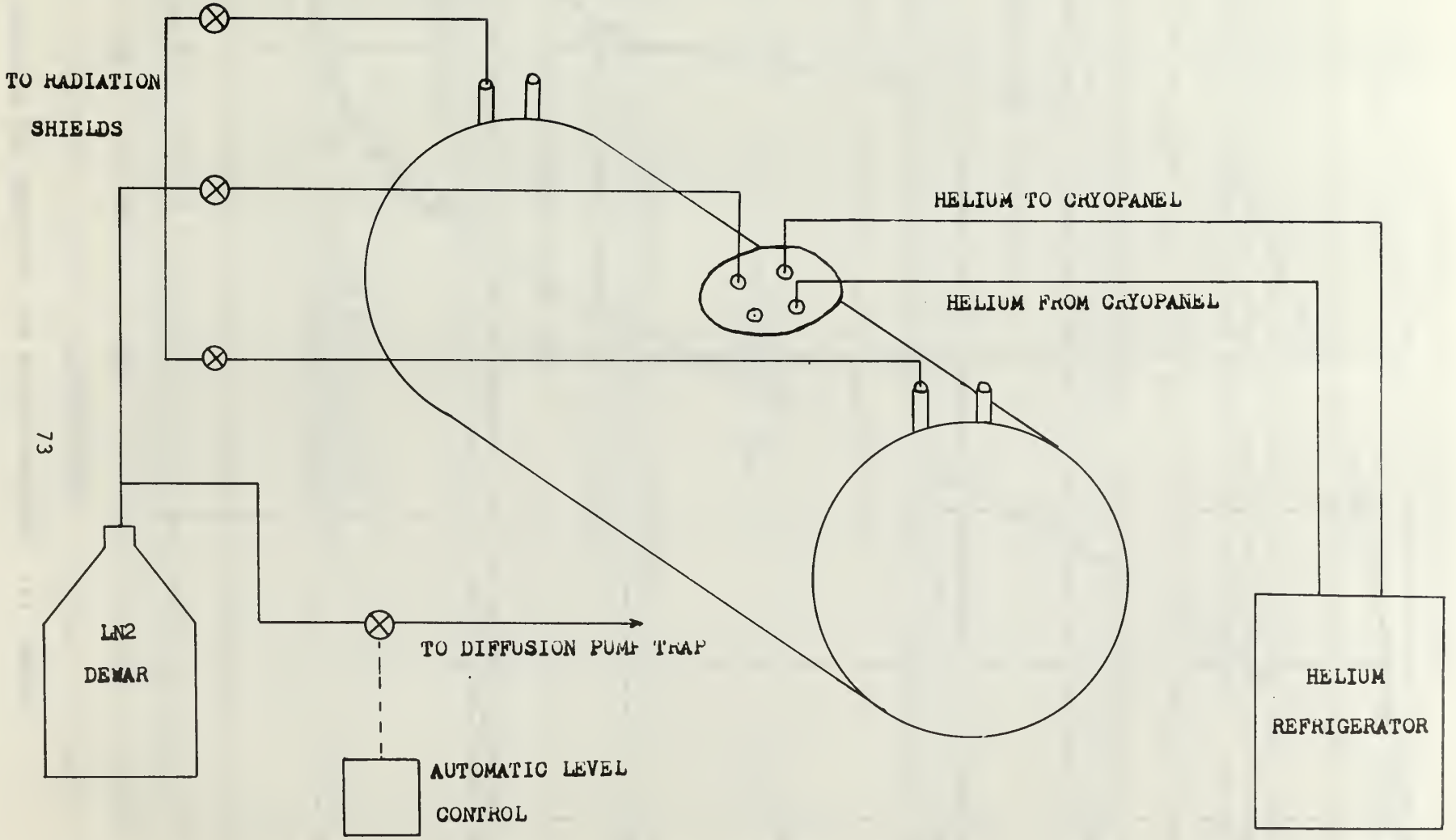

FIGURE 16. CRYOGENIC FLUID TRANSFER SYSTEM

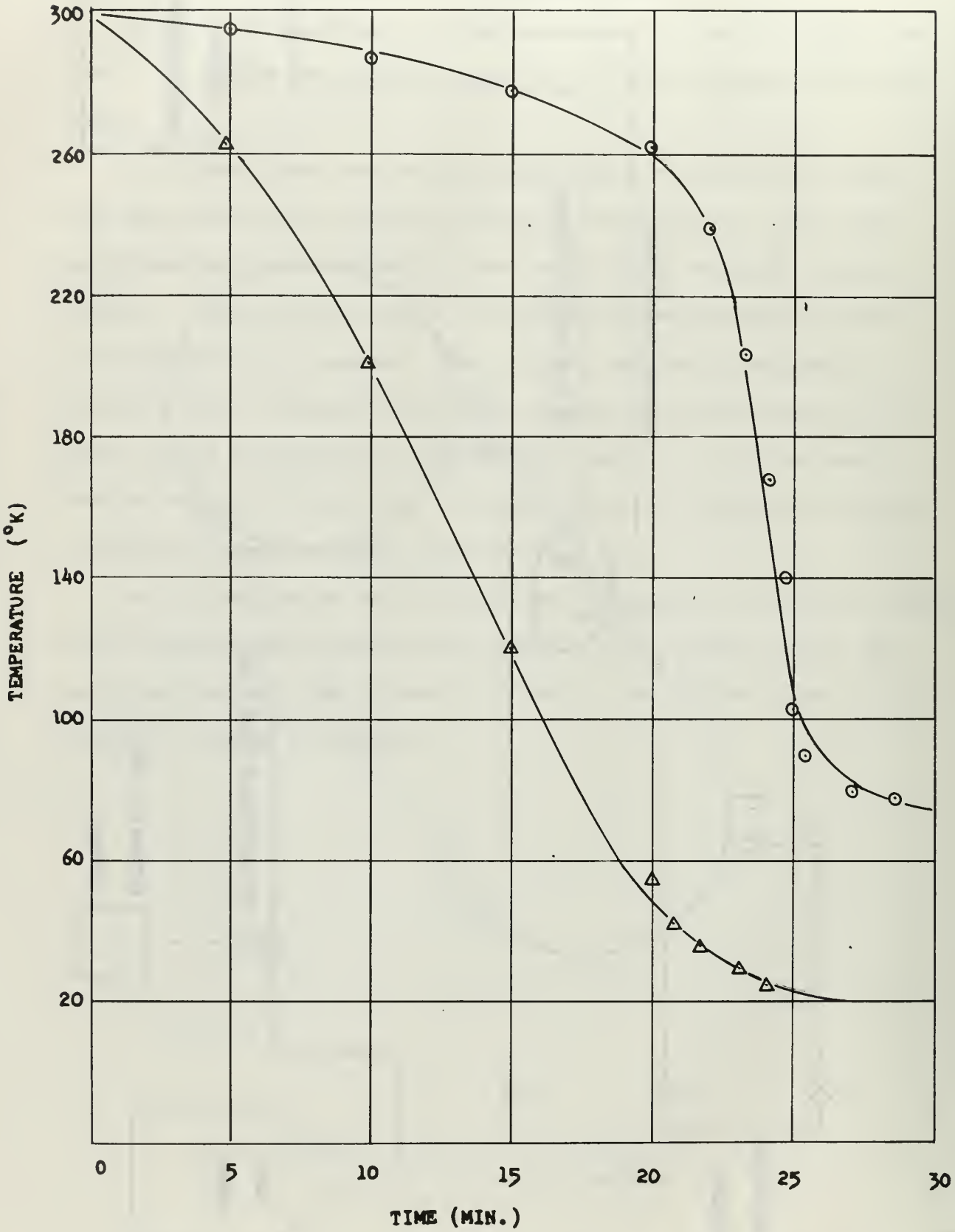

FIGURE 17. COOLDOWN CURVES FOR CRYOPANEL AND SHIELDING

APPENDIX C

Gas Addition and Flow Measurement System

The system used for controlling and measuring the flow of test gas is shown schematically in Figure 18. Of all of the parameters governing the calculation of the capture coefficient, the accurate measurement of the flow of test gas into the system is the most difficult. The amount of flow required depends on the gas temperature, the cryosurface temperature, and the type of test gas used. Since the flows may vary from extremely small to relatively large, the measurement of flow rate can be accomplished in two ways.

Small throughputs may be computed by measurement of the pressure difference across a known conductance in the form of a circular tube. The conductance of the tube can be computed from

$$C = \gamma \frac{\pi}{3} \left(\frac{RT}{2\pi M} \right)^{1/2} \frac{D^3}{L} \qquad \text{(C.1)}$$

where γ is a correction factor for end effects,

D is the inside diameter of the tube, and

L is the length of the tube.

The values of γ can be computed from the equation given by Kennard (20).

$$\gamma = \frac{15\left(\frac{L}{D}\right) + 12\left(\frac{L}{D}\right)^2}{20 + 38\left(\frac{L}{D}\right) + 12\left(\frac{L}{D}\right)^2} \qquad \text{(C.2)}$$

A plot of γ versus L/D is shown in Figure 19. The accuracy of this formula has been verified by Levenson, Milleron and Davis (18) when they used Monte Carlo methods to compute the conductance of a tube and compared their results with carefully measured values. Further verification was

obtained by Landfors and Hablanian (19) when they used this method to compute the pumping speeds of diffusion pumps. The results obtained by Levenson et. al. (18) indicate that the presence of bends in the tube offer very little additional resistance in the molecular flow regime.

The assumptions that must be made for equation (C.1) to hold are:

(a) the flow is steady state with the molecular mean free path longer than the inside diameter of the tube,

(b) the tube must connect effectively infinite volumes, i.e., volumes large enough so that diffuse flow is not inhibited, and

(c) the walls of the tube are microscopically rough so that molecules are diffusely reflected according to the cosine law.

Once the conductance of the tube has been computed, the throughput of the gas can be computed from

$$Q = C(P_1 - P_2) \qquad (C.3)$$

where P_1 is the pressure in an auxiliary vacuum chamber and P_2 is the pressure in the chamber containing the cryopump. The principal uncertainty in determining the throughput by this means is the determination of P_1, since generally $P_1 >> P_2$. To reduce this uncertainty a McLeod gage should be used for $P_1 > 10^{-3}$ torr. For $P_1 < 10^{-3}$ torr, a Bayard-Alpert ionization gage may be used. Although reliance on an ionization gage for absolute measurement is subject to question, the measurement here is relative, i.e., P_1 relative to P_2 in a sequence of observations. Since in such a system the base pressure for zero flow is nearly the same for both gages, the uncertainty in the pressure difference $(P_1 - P_2)$ is less than the uncertainty in either pressure reading alone.

A plot of the molecular conductance is shown in Figure 20 for various ratios of L/D.

This method of measuring throughput is limited by the requirement that the mean free path of the molecules be greater than the inside diameter of the tube. For instance, with a nominal 3/8" tube, P_1 can be no greater than 10^{-2} torr for nitrogen at room temperature or else the mean free path will be such that free molecular flow cannot occur. Figure 21 illustrates the variation of mean free path with pressure for nitrogen.

To accomplish the measurement of larger flows, the rate of pressure rise in a known volume may be measured and the throughput computed from

$$Q = \dot{P}V \qquad (C.4)$$

The system shown in Figure 18 is arranged so as to be able to use either method, as required, to measure the gas throughput. To measure flow using the conductance formula, the system is utilized as follows:

a. Valve #3 is shut, and the variable leak valve is used to set any desired pressure in the auxiliary volume.

b. Valves #1, #2, and the quick acting valve are opened and equations (C.1) and (C.3) are used to compute the throughput from the auxiliary system to the main system.

The system is arranged as follows to measure throughput using the rate of pressure rise in the auxiliary volume.

a. Valves #2 and #3 are shut.

b. Valve #1 is opened and the variable leak valve set to any desired value.

c. The high vacuum valve for the auxiliary system is shut, and the rate of pressure rise in the auxiliary volume is measured.

d. The flow of gas is secured with the gas isolation valve and the auxiliary volume and associated piping are pumped down with the auxiliary pumping system. The variable leak valve must be kept at the value set in step b. of this procedure.

e. Valve #1 is then shut and valve #3 is opened. The flow of gas is re-established by opening the gas isolation valve and flow is now directed to the main vacuum chamber.

In this work, with nitrogen gas and a cryosurface temperature of approximately 25°K, the use of the known conductance of the tube to meter flow resulted in flows so small as to be insignificant for any type of pressure drop measurement. Therefore, only the pressure rise method was used. However, in future work, with variations in the type of test gas and/or higher cryosurface temperatures, the use of a known conductance to meter the flow may result in throughputs which are useful for determining the capture coefficient.

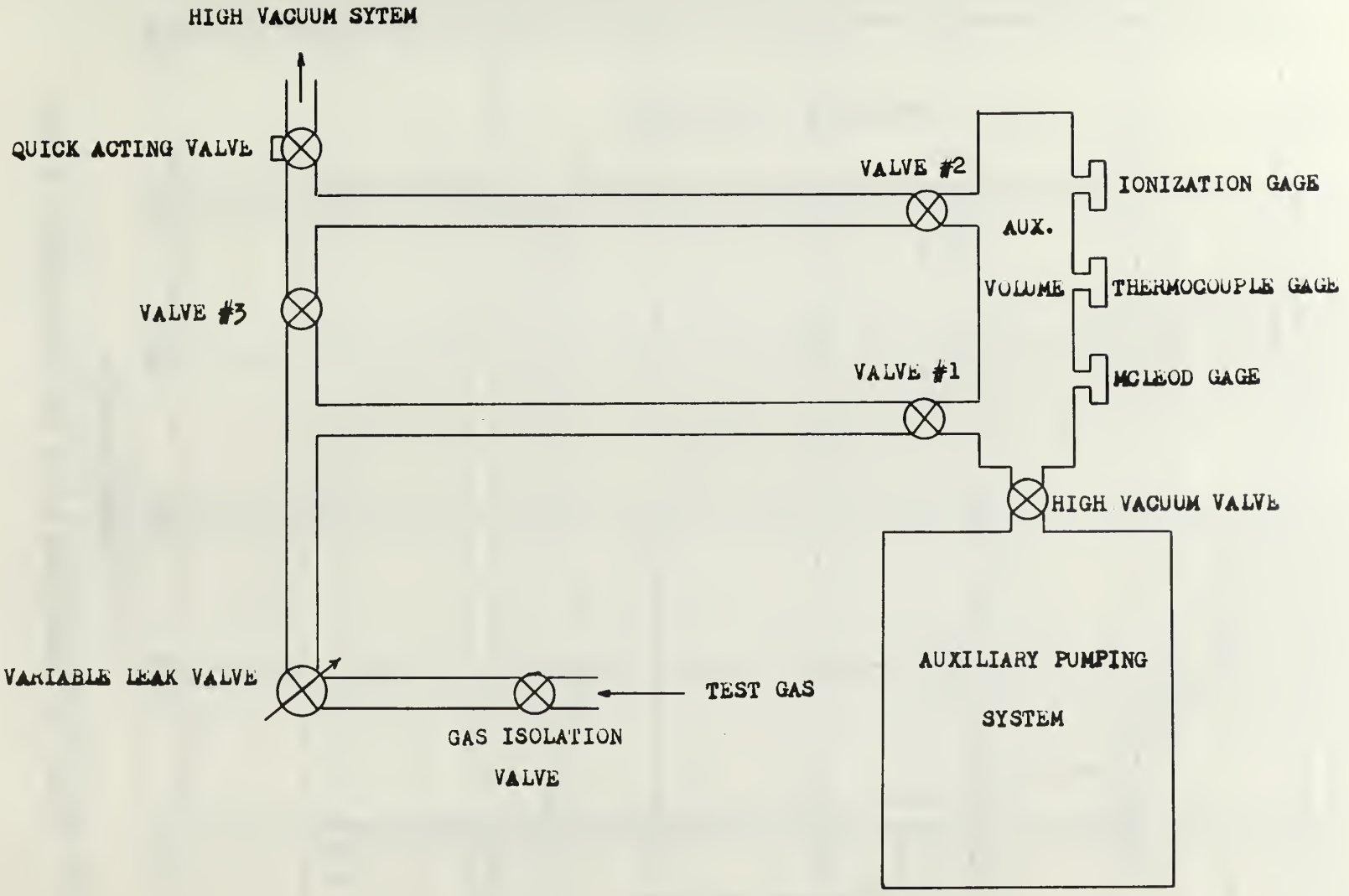

FIGURE 18. GAS ADDITION AND FLOW MEASUREMENT SYSTEM

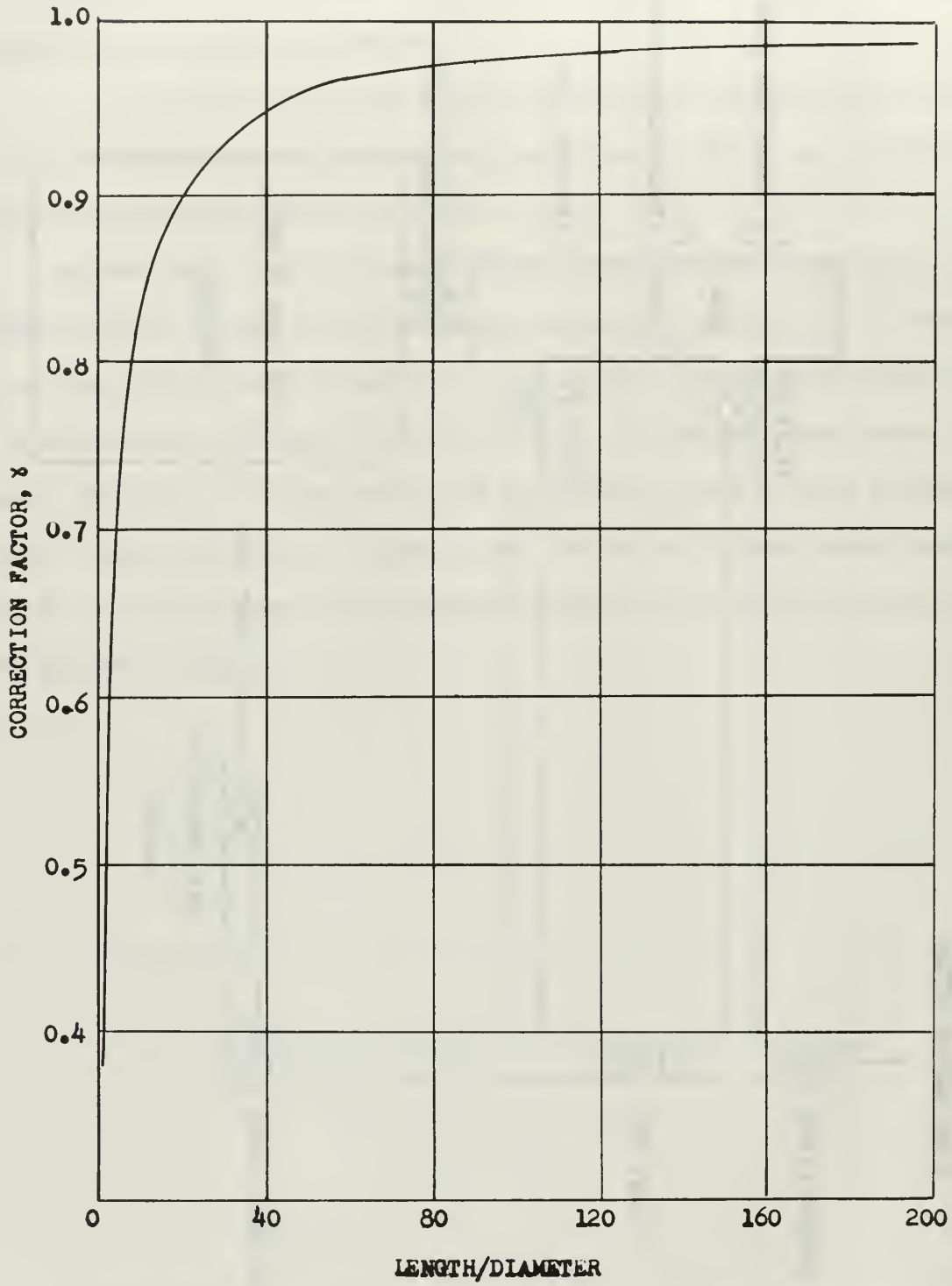

FIGURE 19. CORRECTION FACTOR FOR CONDUCTANCE OF A TUBE

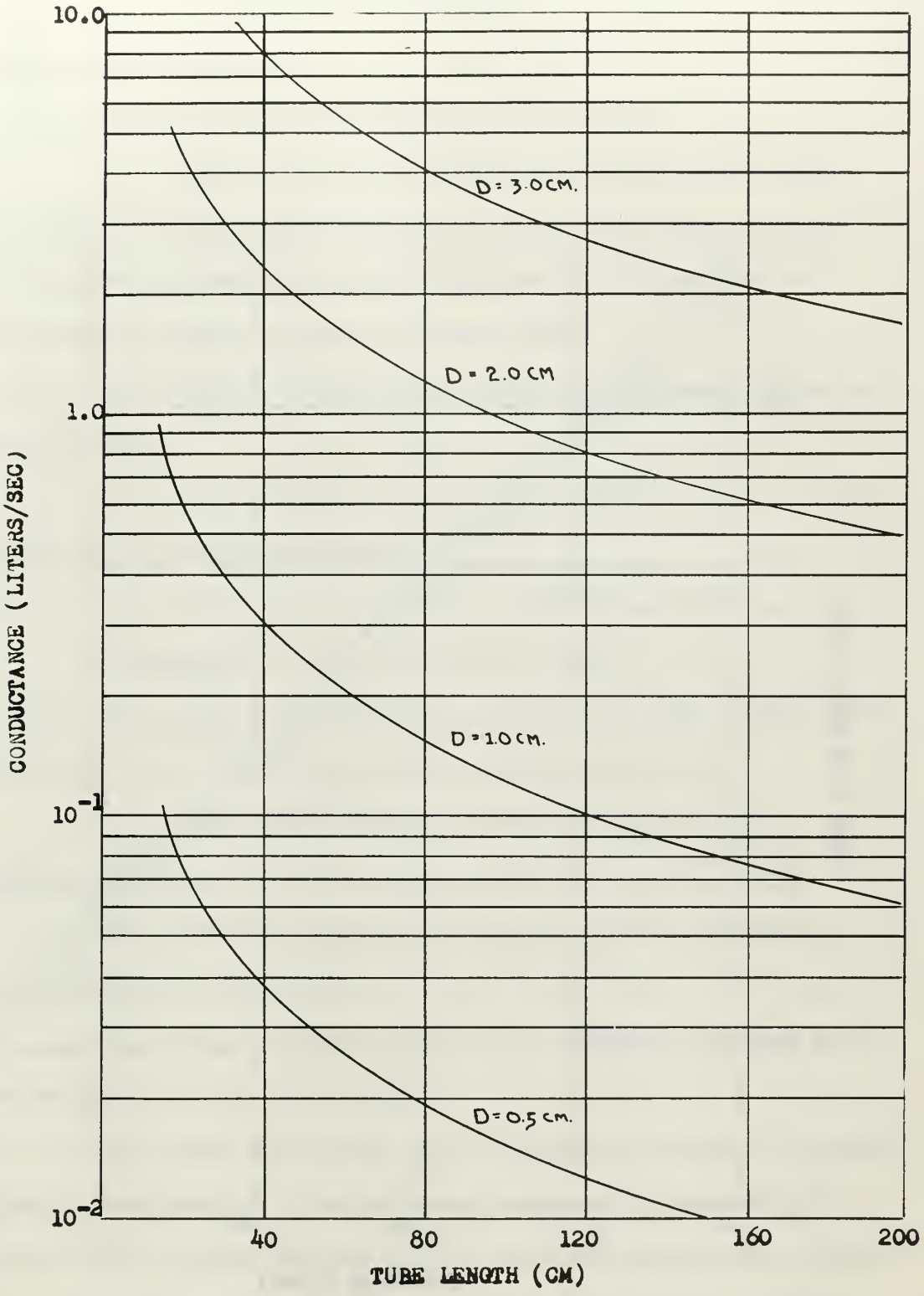

FIGURE 20. CONDUCTANCE OF A CIRCULAR TUBE FOR FREE MOLECULAR FLOW

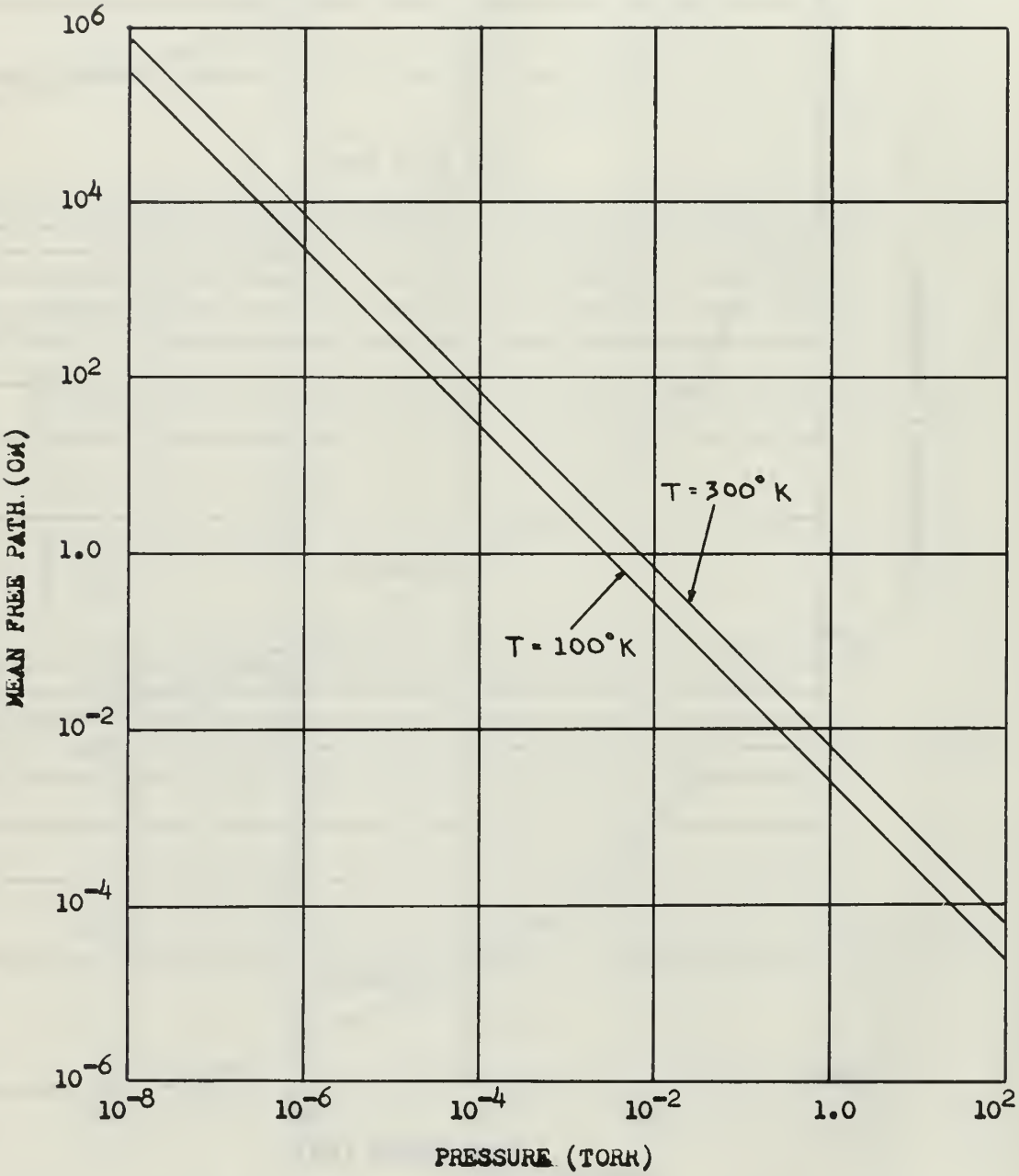

FIGURE 21. MEAN FREE PATH OF NITROGEN

APPENDIX D

Operating Procedures

I. Vacuum System (Figure 13)

A. Initial pumpdown from atmospheric pressure.

1. Check the oil level in the bearing lubricating caps and the pumping chamber of the forepump. Turn on the forepump cooling water. The water is thermostatically controlled at the pump and will not flow unless the pump temperature reaches 180°F.

2. Close disconnect and breakers for forepump, solenoids, and diffusion pump.

3. Open valves for air supply to solenoid valves. Insure air pressure of 90 psig is available.

4. Check that all vent valves, doors and ports are shut.

5. Place overpressure switch on "Out".

6. Energize the solenoids and open the high vacuum valve and the foreline valve. Open the roughing valve manually.

7. Insure quick acting gas addition valve is shut. (Figure 18).

8. Start the forepump and monitor chamber pressure on chamber thermocouple pressure gage.

9. Turn on cooling water to the diffusion pump and cold cap. Insure quick cool valve is shut.

10. When pressure in the tank reaches 70 microns, energize the diffusion pump heaters. The pump requires about 20 minutes to become operational. Monitor the foreline pressure with the foreline thermocouple pressure gage. Initiation of pumping is indicated by a temporary rise in foreline pressure and a rapid decrease in chamber pressure.

11. When the diffusion pump is in operation, shut the roughing valve to prevent backstreaming of forepump oil into the chamber.

12. When the pressure is below 1 micron, energize the ionization gage and monitor tank pressure. Operation is outlined in the manual for the gage controller.

13. When pressure is below 10^{-4} torr, fill the diffusion pump cryogenic trap to reduce backstreaming of diffusion pump oil.

14. When leaving system unattended, place overpressure protection switch on "In".

B. To open the chamber.

1. Shut the high vacuum valve.

2. Open the chamber vent valve.

3. Keep the forepump and diffusion pump operating.

4. When the pressure is equalized, open the chamber.

C. To re-evacuate the chamber.

1. Shut the chamber vent valve.

2. Shut the foreline valve.

3. Open the roughing valve.

4. When the chamber pressure is less than 70 microns, shut the roughing valve, open the foreline valve, open the high vacuum valve.

If the chamber is to be open for only a short period of time, the use of dry nitrogen gas to bring the chamber to atmospheric pressure will considerably reduce the subsequent pumpdown time.

D. To shut the system down completely.

1. Shut the high vacuum valve.

2. De-energize the diffusion pump heaters and turn on the quick cool water.

3. When the diffusion pump is cool, shut the foreline valve and secure the forepump.

4. Open the chamber vent valve and the foreline vent valve to equalize the pressure and then shut these valves.

5. Secure all cooling water.

6. Secure all electrical power.

II. Cryogenic Transfer System.

A. Liquid nitrogen transfer.

1. Connect liquid nitrogen dewar to cryogenic line with rubber tubing.

2. Pressurize dewar to 8 psig with helium.

3. Energize diffusion pump trap automatic level control valve.

4. Insure Armaflex connection fits tightly around supply lines to shields.

5. Open transfer valves and observe exhaust.

6. Monitor thermocouples to check liquid level in the shields.

7. When shields are approximately half full, reduce flow by partially shutting transfer valves. This will help to prevent geysering from the vent lines.

8. It will be necessary to maintain flow to the shields to replace evaporation losses and maintain uniform temperatures.

B. Helium transfer.

1. Pump vacuum jackets on transfer lines to approximately 15 microns.

2. Start and cooldown helium refrigerator.

3. When refrigerator is cool, start the gas transfer.

4. Monitor panel temperature with thermocouples.

III. Flow measurement system (Figure 18).

To use a known conductance to meter flow:

1. Open valves #1, #2, quick-acting valve and auxiliary system high vacuum valve.

2. Shut valve #3 and the variable leak valve.

3. Open the gas isolation valve.

4. With auxiliary pumping system pumping on the auxiliary volume, use the variable leak valve to set the desired pressure in the auxiliary volume.

To measure flow by measuring the rate of pressure rise in the auxiliary volume:

1. Insure gas isolation valve and quick-acting valve are shut.

2. Open valves #1, #2, #3. Open the variable leak valve to the fully open position.

3. Pump down with the auxiliary pumping system.

4. Shut valves #2 and #3.

5. Set variable leak valve to desired setting.

6. Shut auxiliary system high vacuum valve.

7. Open the gas isolation valve and record P versus t.

8. Shut gas isolation valve, open auxiliary system high vacuum valve and pump auxiliary system down as far as possible.

9. Shut valve #1, Open valve #3 and the quick-acting valve.

10. Open the gas isolation valve.

APPENDIX E

Sample Data Reduction

1. To compute the condensation coefficient:

$$f_g = \frac{Q_L \sqrt{T_L}}{A \cdot \Delta P \cdot T_L} \left(\frac{2\pi RT}{M}\right)^{1/2}$$

$$Q_L = \dot{P}_L V_L$$

$V_L = 4.37$ liters

$R = 8.21 \times 10^{7}$ [illegible] $M = 28$ [illegible]

If Q_L is in torr-liters/sec, ΔP in torr and T_g, T_L in °K,

then

$$f_g = 4.41 \times 10^{-4} \frac{Q_L}{\Delta P} \frac{\sqrt{T_L}}{T_L}$$

If Q_L is micron-liters/sec, $\dot{P}_L$ in microns/sec

then

$$f_g = 1.92 \times 10^{-6} \frac{\dot{P}_L}{\Delta P} \frac{\sqrt{T_g}}{T_L}$$

2. To correct for conductance effects:

$$\frac{f^*}{f} = \frac{\beta - f^* A}{\beta}$$

$$f^* = \frac{1}{\frac{1}{f} + \frac{A}{\beta}}$$

$A = 3300\ cm^2$ $\beta = 7180\ cm^2$

$$f^* = \frac{1}{\frac{1}{f} + 0.425}$$

INITIAL DISTRIBUTION LIST

		No. Copies
1.	Defense Documentation Center Cameron Station Alexandria, Virginia 22314	20
2.	Library Naval Postgraduate School Monterey, California 93940	2
3.	Naval Ship Systems Command Navy Department Washington, D. C. 20360	1
4.	Mechanical Engineering Department Naval Postgraduate School Monterey, California 93940	1
5.	Prof. P. F. Pucci Mechanical Engineering Department Naval Postgraduate School Monterey, California 93940	5
6.	LCDR J. A. Bevan, USN Norfolk Naval Shipyard Portsmouth, Virginia 23709	2
7.	LT L. C. Tedeschi, USN Supervisor of Shipbuilding, U. S. Navy Bath Iron Works Bath, Maine	1
8.	LCDR Carl Albero, USN Supervisor of Shipbuilding Bath Iron Works Bath, Maine	1
9.	LCDR George M. LaChance Naval Ship Systems Command Code 1500 Navy Department Washington, D. C. 20360	1

DOCUMENT CONTROL DATA - R&D

(Security classification of title, body of abstract and indexing annotation must be entered when the overall report is classified)

1. ORIGINATING ACTIVITY (Corporate author) Naval Postgraduate School Monterey, California 93940	2a. REPORT SECURITY CLASSIFICATION Unclassified 2b. GROUP

3. REPORT TITLE

Capture Coefficients of Nitrogen on a Cryogenically Cooled Panel

4. DESCRIPTIVE NOTES (Type of report and inclusive dates)

5. AUTHOR(S) (Last name, first name, initial)

BEVAN, John Albert, LCDR

6. REPORT DATE	7a. TOTAL NO. OF PAGES	7b. NO. OF REFS
June 1967	86	20

8a. CONTRACT OR GRANT NO.	9a. ORIGINATOR'S REPORT NUMBER(S)
b. PROJECT NO.	
c.	9b. OTHER REPORT NO(S) (Any other numbers that may be assigned this report)
d.	Approved for public release; distribution unlimited.

10. AVAILABILITY/LIMITATION NOTICES

~~This document is subject to special export controls and each transmittal to foreign nationals may be made only with prior approval of the Naval Postgraduate School.~~

11. SUPPLEMENTARY NOTES	12. SPONSORING MILITARY ACTIVITY

13. ABSTRACT

The pressure drop method was used to experimentally determine the capture coefficients of nitrogen gas on a flat cryopanel maintained at a temperature of 25°K. The capture coefficients for 300°K nitrogen varied from a maximum of 0.70 for low system gas loads to a minimum of 0.10 for high system gas loads.

DD FORM 1 JAN 64 1473

14 KEY WORDS	LINK A		LINK B		LINK C	
	ROLE	WT	ROLE	WT	ROLE	WT
Capture coefficient						
Nitrogen gas						
Cryopumping						
High Vacuum						